


PAIRBOT: A NOVEL MODEL FOR AUTONOMOUS MOBILE ROBOT SYSTEMS CONSISTING OF PAIRED ROBOTS

A PREPRINT

 **Yonghwan Kim**
Department of Computer Science
Nagoya Institute of Technology
Aichi, Japan
kim@nitech.ac.jp

 **Yoshiaki Katayama**
Department of Computer Science
Nagoya Institute of Technology
Aichi, Japan
katayama@nitech.ac.jp

 **Koichi Wada**
Department of Applied Informatics
Hosei University
Tokyo, Japan
wada@hosei.ac.jp

October 10, 2024

ABSTRACT

Programmable matter (PM) is a form of matter capable of dynamically altering its physical properties, such as shape or density, through programmable means. From a robotics perspective, PM can be realized as a *distributed system consisting of numerous small computational entities* working collaboratively to achieve specific objectives. Although autonomous mobile robot systems serve as an important example and have been researched for more than two decades, these robots often fail to perform even basic tasks, revealing a considerable gap in PM implementation.

In this paper, we introduce a novel computational paradigm, termed the Pairing Robot model (*Pairbot model*), which is built on an autonomous mobile robot system. In this model, each robot forms a *pair* with another, enabling them to recognize each other and adapt their positions to achieve designated goals. This fundamental principle of *pairing* substantially enhances inter-robot connectivity compared to conventional *LCM*-type model, even under asynchronous scheduler conditions. This shift has considerable implications for computational capabilities, specifically in problem solvability.

We explore two specific challenges—the *perpetual marching* problem and the *7-pairbots-gathering* problem—to demonstrate the computational power of *Pairbot model*. This model provides new avenues and insights to address inherent issues in autonomous mobile robots.

Keywords pairbot · programmable matter · autonomous mobile robots · LCM model

1 Introduction

1.1 Background

The foundational concept of a distributed system composed of multiple robots was initially introduced in a landmark paper Suzuki and Yamashita [1999]. Within this framework, each robot autonomously observes the positions of the other robots and moves to a new position based on a prescribed algorithm. These robots are anonymous (i.e., indistinguishable in appearance) and uniform (i.e., executing identical algorithms). In the work cited Suzuki and Yamashita [1999], this conceptual model for mobile robots is designated as the *LCM (Look-Compute-Move) model*. For simplicity, we will refer to robots operating under the conventional *LCM* model without specific assumptions such as *light* Das et al. [2015] as *LCM-robots*. The paper provides a comprehensive analysis of the capabilities and constraints of this distributed system, exploring issues such as pattern formation and agreement problems. Since the introduction of the *LCM* model, much related work has been studied to clarify its computational power and limitations Flocchini et al. [2019], Prencipe [2014] for more than 20 years.

Numerous studies have focused primarily on the relationship between the computational capabilities of each robot and the solvability of the given problem, such as problems of gathering Cicerone et al. [2018], Cieliebak et al. [2012],

pattern formation Flocchini et al. [2008, 1999], Fujinaga et al. [2015], Yamauchi et al. [2017], and flocking Gervasi and Prencipe [2004], Souissi et al. [2009].

Thus, defining the necessary (possibly minimum) capabilities to solve the given problem is an essential issue. Many capabilities of a robot (e.g., geometric agreement, scheduler, visibility, and transparency) should be considered to solve a problem, and it has been shown that the solvability of each problem depends deeply on these capabilities. Clarifying the capabilities required for the given problem has many advantages, including cost reduction, scalability, and fault tolerance. Therefore, various distributed coordination problems for autonomous mobile robots are still widely studied in many fields, such as robotics, engineering, and medical science.

1.2 Related Work

Building on the seminal work by Suzuki and Yamashita Suzuki and Yamashita [1999], which introduced the autonomous mobile robot model and explored its computational capabilities, extensive research has since been investigated concerning its computational power and limitations of these robots in various distributed coordination tasks, such as rendezvous Izumi et al. [2011], gathering Cicerone et al. [2018], Cieliebak et al. [2012], pattern formation Flocchini et al. [2008, 1999], Fujinaga et al. [2015], dispersion Kshemkalyani et al. [2020], Molla et al. [2021], Augustine and Moses [2018], Barriere et al. [2009], and flocking Gervasi and Prencipe [2004], Souissi et al. [2009].

In the early years of the study, robots are modeled as points (i.e., without volume). However, many recent studies consider robots that have volume, known as *fat robots* Czyzowicz et al. [2009], or opaque robots (each robot may obstruct the view of the other robots): these models present new paradigms for problems such as the complete visibility problem Aljohani et al. [2018], Kim et al. [2023]. Many studies aim to clarify the relationship between robots' capabilities and the solvability of various problems Flocchini et al. [2019], Prencipe [2014], Buchin et al. [2021].

Programmable matter (PM), which is defined as a matter that can change its physical properties, such as shape, color, and stiffness, in response to a computer program, was first introduced in Toffoli and Margolus [1993], Goldstein et al. [2005]. Realizing programmable matter could bring several potential advantages, including: (1) **flexibility**; PM makes matters highly flexible and adaptable, which allows PM to be used in a variety of applications such as wearable devices and soft robotics Bongard [2013], Kim et al. [2013], (2) **customization**; PM could allow customization of objects and devices to meet specific needs and requirements, e.g., tailored clothing or customized prosthetics, and (3) **interactivity**; PM could bring new levels of interactivity and responsiveness to physical objects, e.g., objects that respond to touch, sound, or light in creative ways. These potential benefits of PM are significant and could lead to many new and innovative applications. However, PM is a complex and challenging task that requires solving several technical and scientific problems, and thus it is still in the research stage in various fields such as robotics, computer science, and material science. PM can be implemented through the use of small robots, such as nanorobots Cerofolini et al. [2010], Yarin [2010], that can work together to form larger structures. Many studies on autonomous mobile robot systems have the potential to be useful in realizing PM. However, autonomous mobile robots require various additional capabilities in many cases, and some of them are not necessarily realistic, as they have many difficulties, even in simple problems.

As a new computational model for the realization of programming matter, a self-organizing particle system, called *Amoebot model*, was first introduced in Derakhshandeh et al. [2014]. The *Amoebot* model consists of a large number of computational *particles* placed on a triangular grid plane, which locally interact with each other to solve problems. Each particle repeatedly changes its state to *contraction* or *expansion*, which means the state by which a particle occupies one node and two adjacent nodes. The *Amoebot* model allows for coordinated movement between two connected particles, called *handover*. A handover is an interaction in which a particle can contract out of a certain node at the same time that another particle expands into that node. The *Amoebot* model can solve various distributed coordination problems, such as the universal coating problem Daymude et al. [2017a], leader election Bazzi and Briones [2019], Daymude et al. [2017b], and convex hull formation Daymude et al. [2020]. Furthermore, recent work has introduced the *canonical amoebot model*, which considers concurrent control Daymude et al. [2021].

SILBOT model D'Angelo et al. [2020] is another computational model for PM that introduces a new modeling approach by relaxing some of the assumptions made in the previous model. In the *SILBOT* model, each particle cannot communicate with the others (i.e., silent) and operates asynchronously (i.e., in full synchronicity). However, this model requires a specific symmetry-breaking capability; if two or more particles attempt to expand toward the same cell, only one of them succeeds. The literature D'Angelo et al. [2020] shows that a leader election can be achieved from a connected configuration with certain restrictions (or with some additional assumptions).

MOBLOT Cicerone et al. [2021] is a computational model designed from a different point of view, which extends the oblivious mobile robot model to address a wider spectrum of cases. The main difference of the *MOBLOT* model is heterogeneous system; all (oblivious) robots are partitioned into 2 types, colored black or white. This feature enables simple (oblivious) robots to perform more complex tasks.

The literature Daymude et al. [2021], D’Angelo et al. [2020], Cicerone et al. [2021] shows that these new computational models for PM have great computational power in some problems; however, they require some different assumptions which are not considered (or cannot be used) in the conventional autonomous mobile robot model, such as explicit communication or handover. Here, we expect that if we can design a new computational model as close as possible to the conventional *LCM* model Suzuki and Yamashita [1999], we can use many results among many existing results investigated for a long time.

1.3 Comparison with the Other Computational Models

Here we provide a comparison between our proposed model *Pairbot model* and three other computational models: *Amoebot*, *SILBOT*, and *MOBLOT*. It is important to note that these models solve different problems based on different assumptions; thus, it is difficult to provide a direct comparison of their computational power.

The *Amoebot* model is one of the most popular PM models. Various *Amoebot* models presented in many studies have recently been generalized in Daymude et al. [2021], and it is currently one of the most promising models for PM. It relies on explicit communication (message passing) between particles, allowing them to move in coordinated ways, form complex structures, and perform various tasks. The most notable feature of the *Amoebot* model is the solvability of the leader election; the communication between particles is a very useful capability to solve the leader election problem. In many cases, the *Amoebot* model uses the leader elected among the particles to solve the pattern formation problem Luna et al. [2020], Derakhshandeh et al. [2015]. The ability to elect the leader under the various assumptions is one of the strongest computational power of the *Amoebot* model.

The *SILBOT* model D’Angelo et al. [2020] (as in *Silent robot*) relaxes several assumptions, especially communication capacity. G. D’Angelo et al. show that a leader election, at most three leaders could be elected due to the symmetry of the initial configuration, can be achieved by this model without any communication from any simple (i.e., without holes) connected configuration. As one of the features of *SILBOT*, it assumes 2-hop visibility; each particle can detect nodes within 2 hops. To our knowledge, only the leader election problem is investigated under the *SILBOT* model D’Angelo et al. [2020], however, this study shows that the leader election is solvable without any explicit communication under some specific model. Although it is difficult to compare the computational power between *Amoebot* and *SILBOT*, it is natural to say that *Amoebot* is stronger than *SILBOT* if there is no additional assumption.

The *MOBLOT* model is a computational model based on the *LCM* model; thus, robots are silent (without explicit communication) and do not have special symmetry-breaking capabilities like *SILBOT*. Therefore, *MOBLOT* is the model closest to our proposed model *Pairbot model*: These two computational models are designed with the goal of significantly changing their computational power by adding a few assumptions to conventional mobile robots. *MOBLOT* is a model inspired by molecules in which oblivious autonomous mobile robots with some different roles are combined to act as a new large computational entity; such as atoms, molecules are formed. The robots in the same molecules can operate together, e.g., they have geometric agreement, and this enables the robots to break their symmetry because the robots forming molecules become nonequivalent (i.e., there is no symmetry). The literature Cicerone et al. [2021] gives one special case study of pattern formation, named matter formation, to form molecules by robots. However, this study provides us with the fact that this model can enlarge the class of achievable patterns of oblivious mobile robots that break the symmetry of the system. Since *MOBLOT* is based on conventional mobile robots, it is a relatively weak computational model compared to the two models above, but assumes relatively strong capabilities (even though they are not unrealistic) compared to our proposed model; *Pairbot model* assumes only the unique pair of each robot, which can be easily implemented (or simulated) with some previous assumptions, such as lights.

The Uniqueness of Pairbot model: What separates *Pairbot model* apart is its minimalistic approach to computational capabilities, namely the unique pairing of each robot. The real strength of *Pairbot model* lies in its *connectivity*, even under asynchronous schedulers, as shown in our solutions to the problems of *perpetual marching* and *7-pairbots-gathering*. The former illustrates that a problem unsolvable by LCM-robots under a semi-synchronous scheduler is, in fact, solvable by *pairbots* under an asynchronous scheduler. The latter shows how *Pairbot model* outperforms traditional robots in terms of visibility range. This clearly highlights the superior efficiency of *Pairbot model* in solving problems with fewer assumptions, offering advantages in terms of implementability and real-world applicability.

In summary, while *Amoebot* offers the most computational power, followed by *SILBOT* and *MOBLOT* (these two models are hard to compare), *Pairbot model* carves out its own unique space by efficiently solving problems with fewer computational assumptions. This makes it an ideal choice for scenarios where computational simplicity and efficiency are critical.

1.4 Contribution

In this paper, we introduce a novel method for implementing programmable matter, designed to simplify the exploration and analysis of its capabilities using established knowledge. Our model, known as *Pairbot model*, features two robots that operate collaboratively as a pair on a triangular grid. The *Pairbot model* introduces a unique feature called an *exclusive move*, which is absent from the traditional *LCM* model. Despite this addition, *Pairbot model* largely retains the functionalities found in the *LCM* model. This newly added capability significantly enhances computational power, specifically problem solvability, and offers valuable insights into the realization of programmable matter based on the *LCM* model.

In *Pairbot model*, each robot is uniquely paired with another robot, referred to as *buddy*. We denote these paired robots as *pairbot*, and a *pairbot* system comprises two or more *pairbots*. Every robot in a *pairbot* can identify its *buddy*. The paired robots repeatedly alter their geometric relationships, *short* and *long*, to achieve their objectives. In the *short* state, both robots share the same spatial point, while in the *long* state, they occupy adjacent points.

To elucidate the functioning of *pairbot*, we present two challenges: the *perpetual marching* and the *7-pairbots-gathering* problems. The former problem is not solvable by *LCM*-robots under a semi-synchronous scheduler, and latter is not solvable by *LCM*-robots with visibility range 1. We propose two deterministic algorithms as solutions for these challenges, which serve to demonstrate how *pairbots* operate and both the computational power and the limitations of the *Pairbot model*. In particular, the first algorithm solves the perpetual marching problem under an asynchronous scheduler, and the second solves the *7-pairbots-gathering* problem by *pairbots* with visibility range 1.

1.5 Paper Organization

The rest of this paper is organized as follows: Section 2 introduces the proposed system model, called *Pairbot model*; Section 3 gives the *perpetual marching* problem and proposes an algorithm to solve this problem; Section 4 discusses another problem, called the *7-pairbots-gathering problem* and an algorithm to solve this problem; and finally Section 5 concludes the paper.

2 Proposed Model: *Pairbot model*

2.1 Triangular Grid Plane

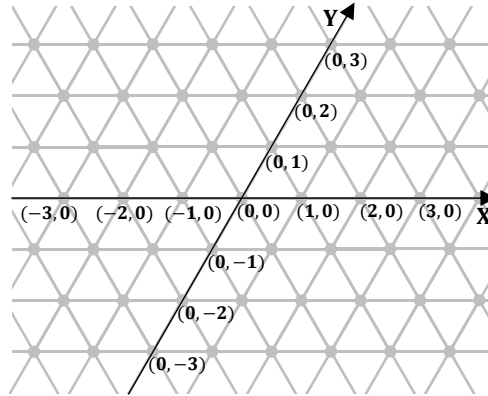


Figure 1: Triangular grid plane \mathbb{T}

We consider a set of n autonomous mobile robots denoted by $R = \{r_1, r_2, \dots, r_n\}$ on a two-dimensional triangular grid plane $\mathbb{T} = \mathbb{Z}^2$ (Figure 1). The distance between two points u and v in \mathbb{T} is defined by the following equation:

$$dist(u, v) = \begin{cases} |u.x - v.x| + |u.y - v.y| & \text{if } (u_x - v_x)(u_y - v_y) \geq 0 \\ \max(|u.x - v.x|, |u.y - v.y|) & \text{otherwise} \end{cases} \quad (1)$$

If the distance between two points is one, the two points are *adjacent*. The triangular grid plane \mathbb{T} can also be represented as an infinite regular graph $G_{\mathbb{T}} = (V_{\mathbb{T}}, E_{\mathbb{T}})$, where $V_{\mathbb{T}}$ consists of all points on \mathbb{T} and $E_{\mathbb{T}}$ is defined by all two adjacent points on \mathbb{T} (i.e., for $u, v \in V_{\mathbb{T}}$, $(u, v) \in E_{\mathbb{T}}$ iff $dist(u, v) = 1$).

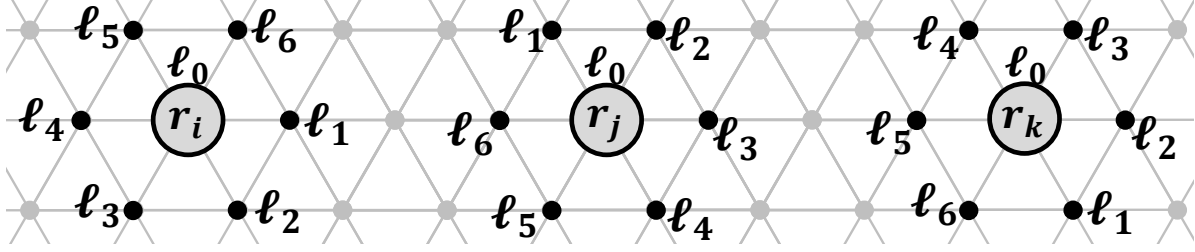


Figure 2: Example of the local labels of each robot without any geometric agreement

Note that we can use the function $dist()$ for robots such as $dist(r_i, r_j)$ which is equal to $dist(u, v)$ where u (resp. v) is the point occupied by r_i (resp. r_j).

2.2 Geometric Agreement

Every robot has its own local coordinate system that can be defined by *directions* (i.e., X and Y axes) and *orientations* (i.e., positive and negative sides) of each axis. We can consider some levels of consistency among robots on their local compass: *total agreement*, when all robots agree on the directions and orientations of both axes; *partial agreement*, when all robots agree on the direction and orientation of only one axis or on the *chirality*, which means a sense of axis orientation (i.e., clockwise or counter-clockwise); or *no agreement*, when no agreement exists among the local coordinate system of each robot. In the problems considered in this paper, we assumed *no agreement* and *total agreement* respectively. Note that the latter means that all robots in R agree on the directions and orientations of both axes, but no robot agrees on the position of the origin. In other words, no robot knows its global coordinate, but all agree on the sense of direction (e.g., north, south, east, and west).

2.3 Pairbot

In *Pairbot model*, every robot has its unique partner, called *buddy*: robot r_i is the *buddy* of robot r_j if and only if robot r_j is the *buddy* of robot r_i . In this case, we call the two robots r_i and r_j a *pairbot*. The *buddy* of each robot is initially determined and never changed. Obviously, the number of robots n is an even number.

2.3.1 Operations

Each robot r_i cyclically performs the following three operations: *Look*, *Compute*, and *Move* based on a well-known computational model (LCM model Suzuki and Yamashita [1999]).

- *Look*: Each robot takes a snapshot consisting of robots within the visibility range with respect to its local coordinate system.
- *Compute*: Each robot performs a local computation based on the snapshot taken by the *Look* phase according to Algorithm \mathcal{A} . As a result of the *Compute* phase, each robot determines its destination point to move.
- *Move*: Based on the result of the *Compute* phase, each robot actually moves to the adjacent destination point from the current point in the *Move* phase. A null movement (staying) is allowed (i.e., a robot does not move).

2.3.2 Local Label

Each robot locally maintains the labels for each incident edge (from ℓ_1 to ℓ_6) to distinguish its adjacent points. Each robot selects one adjacent point and labels the point as ℓ_1 , and labels the other points from ℓ_2 to ℓ_6 in clockwise order (based on its local chirality). The label ℓ_0 represents its current point. Note that the direction located the point labeled by ℓ_1 may be different by the assumption of geometric agreements among robots. Moreover, the clockwise order may also vary by the assumption of *chirality*.

Figure 2 represents an example of the local labels of three robots, r_i , r_j , and r_k , where there is *no agreement* among the robots. In this figure, robot r_i labels the point on the right side as ℓ_1 ; however, robot r_j or r_k labels the point at a different direction with r_i 's as ℓ_1 because robots do not agree on the directions and orientation of any axis. Moreover, the edges of robot r_k are labeled in counterclockwise order, because neither do the robots agree on chirality.

In the problems discussed later in this paper, we assume either *no agreement* or *total agreement* depending on the problems.

2.3.3 Capabilities

All robots are oblivious (i.e., do not have memory), which means that they do not know any of their past executions.

Each robot can recognize other robots within *visibility range* V . This means that each robot can sense only up to V hops far from itself. In other words, the robot r_u at the point u and the robot r_v on point v , where $r_u, r_v \in R$ and $u, v \in V_{\mathbb{T}}$, can observe each other only when $\text{dist}(u, v) \leq V$. We assume here that the *visibility range* of each robot is one (i.e., each robot can observe only the robots at the adjacent points).

We also assume that each robot has the capability of *weak multiplicity detection*, that is, each robot can distinguish from the following three cases at points within its visibility: no robot exists; only one robot exists; and more than one robot exists. Note that if each robot can count the exact number of robots that occupy the point within its visibility range, this is *strong multiplicity detection*.

All robots in R are *anonymous*: each robot has no identifier and no robot is distinguishable by its appearance. However, each robot maintains the position of its *buddy* using its local label, implying that each has a local memory to maintain the position (local label) where its *buddy* is located.

We further assume here that when a *pairbot* occupies the same point, only one robot can move to its adjacent point when it moves. We call this an *exclusive move*. Note that no robot knows if any other two robots are *pairbot* or not.

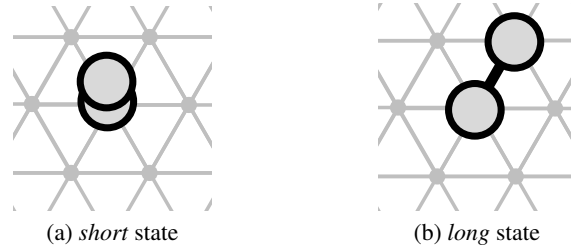


Figure 3: Two states (positional relation) of two robots in the same pair

The two robots in one *pairbot* occupy the same point or two adjacent points on \mathbb{T} (Figure 3). We call the former one a *short state* and the latter a *long state*. When a *pairbot* is in a *short state*, only one robot in the *pairbot* can (exclusively) move the adjacent point from its current point, and the *pairbot* becomes a *long state*. When a *pairbot* is in a *long state*, either of the two robots can move to the point occupied by its *buddy*, and the state is changed back to a *short state*. In the *Pairbot model*, every *pairbot* repeatedly changes its state to *short* and *long* to achieve the goal. A *pairbot* never knows which robot moved while its state changes because all robots are oblivious.

Figure 4 illustrates an example of *pairbots*. *Pairbot* r_i and r_j is in a *long state*, and some other robots are placed at the other points in \mathbb{T} . In this case, robot r_i recognizes that its *buddy* is robot r_j on its right side. However, r_i cannot know the pair relations of the other robots (e.g., robot r_i never knows the *buddy* of robot r_x on its lower left side). The robot r_y can recognize that another robot is at the same point due to *weak multiplicity detection*. Furthermore, r_y can know that the *buddy* r_x is on the point of its upper left side and is in a *long state*.

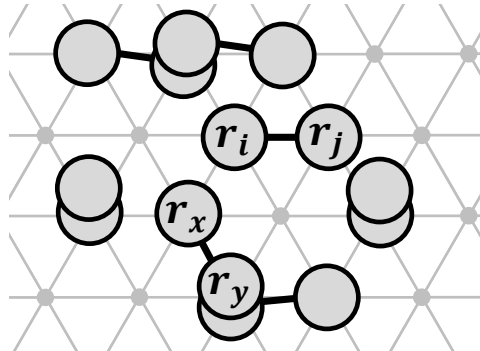


Figure 4: An example of *pairbots*

2.4 Scheduler

We consider a *scheduler* that decides which robot to *activate* and the *timing* of each operation. A scheduler has three representative assumptions (models): *fully-synchronous* (FSYNC); *semi-synchronous* (SSYNC); and *asynchronous* (ASYN).

In an FSYNC scheduler, all robots are activated at the same time, and the three operations of *Look*, *Compute*, and *Move* are executed based on exactly the same cycle time. In an SSYNC scheduler, all robots perform their operations at the same time, but some may not be activated. The robots, which are not activated by a scheduler, wait until all activated robots terminate their operations. Lastly, in an ASYN scheduler, no assumption on the cycle time of each robot is provided, implying that all robots execute their operations at unpredictable time instants and durations.

We assume herein an ASYN scheduler such that the *Move* phase operates atomically: each robot requires an unpredictable finite time to operate in the *Look* or *Compute* phase, but it can atomically move in a property called the *move-atomic property*. Therefore, each robot is never observed while moving. We assume that the two robots, which are a *pairbot* are activated at the same time by the scheduler.

2.5 Configuration

A *configuration* C_t consists of the positions of all robots in R at time t : $C_t = \{(r_1.x(t), r_1.y(t)), (r_2.x(t), r_2.y(t)), \dots, (r_n.x(t), r_n.y(t))\}$, where $(r_i.x(t), r_i.y(t))$ is the global coordinate of robot r_i at time t on \mathbb{T} . Note that no robot knows its global coordinate on \mathbb{T} . Let R' be a non-empty subset of R and let \mathcal{A} be an algorithm. We denote $C_t \mapsto_{(R', \mathcal{A})} C_{t+1}$ if a configuration C_{t+1} is obtained when each robot in R' simultaneously performs its *Move* operation of \mathcal{A} in configuration C_t . Hence, a scheduler can be presented as an infinite sequence R_1, R_2, \dots of nonempty subsets of R . An execution $\Xi_{\mathcal{A}}(S, C_0)$ of Algorithm \mathcal{A} along the schedule $S = R_1, R_2, \dots$ starting from configuration C_0 , where C_0 is an initial configuration, can be defined as the infinite sequence of configurations C_0, C_1, \dots such that $C_i \mapsto_{(R_{i+1}, \mathcal{A})} C_{i+1}$ for all $i \geq 0$.

3 The Perpetual Marching Problem

3.1 Problem Definition

In this section, we consider the *perpetual marching problem*, which is an infinite linear movement of *pairbots* without any geometrical agreement (i.e., they do not have any common sense of direction).

We now define the marching problem as follows:

Definition 1 Perpetual Marching Problem. Algorithm \mathcal{A} solves the perpetual marching problem if there is a well-initiated configuration C_{init} , a certain direction \mathcal{D} , a constant k , and an infinite execution $\Xi_{\mathcal{A}}(S, C_{init})$ such that after each (constant) t steps, all robots move to a point that is a distance of k toward the direction \mathcal{D} .

Intuitively, when locating the robots in a predetermined configuration (a well-initiated configuration C_{init}), an algorithm makes all the robots to move infinitely (an infinite execution) at a constant speed (a constant k) in a specific direction (a certain direction \mathcal{D}). Figure 5 illustrates an example of perpetual marching.

It is worthwhile to noting that the perpetual marching requires a fixed distance movement within a constant speed. In other words, a movement in a specific direction within a finite time is not feasible perpetual marching. For instance, a movement such as a perpetual exploration while expanding the range (refer to Figure 6(a)) or a repetitive movement back and forth (refer to Figure 6(a)) is not feasible in the perpetual marching problem, because from the perspective of moving in a fixed direction, their speed progressively decreases. On the other hand, whether the movement is in a straight line (refer to Figure 7(a)) or follows a zigzag path, (refer to Figure 7(b)) it becomes a feasible perpetual marching as long as it maintains a constant speed.

3.2 Perpetual Marching Algorithm

First we introduce an well-initiated configuration C_{init} as Figure 8. Figure 9 shows the proposed algorithm (using graphical representation) consisting of 7 rules when configuration C_{init} is given. The detailed pseudocode of the algorithm is provided in the next section. In each rule, the circle in the center represents the grid point where a robot (who executes the algorithm) exists and 6 other circles present adjacent grid points. Each number shows the number of robots and a black circle represents the point where the *buddy* exists. It is worth to noting that even if there are three or more robots at one point, the number (of robots) becomes 2 due to the weak multiplicity. Moreover, these rules are

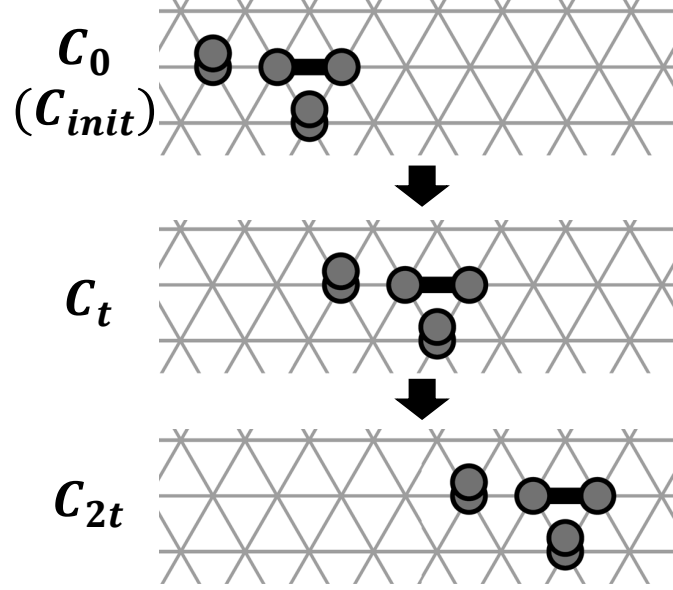


Figure 5: An example of perpetual marching

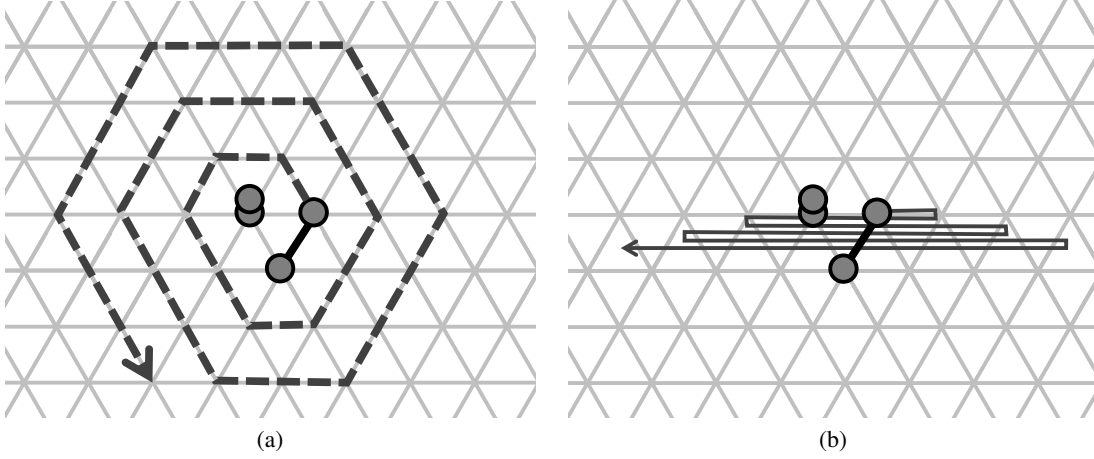


Figure 6: Examples of non-feasible perpetual marching

applied as the same rules even mirrored and/or rotated because robots do not agree on any axis nor chirality. If the observation result of the robot satisfies any of these conditions, the robot moves to the point indicated by a black arrow. Note that the direction to move is uniquely determined in each rule, thus every robot can move to the correct direction without a sense of direction.

During the execution of the algorithm, eight different configurations appear sequentially. After 8 steps, the initial configuration appears again with a shift of distance one to the right direction. These 8 steps are infinitely repeating and the perpetual marching is achieved. As a result, the following corollary holds.

Lemma 1 *The proposed algorithm solves the perpetual marching problem under an ASYNC scheduler.*

Proof 1 *In configuration C_{init} , there exists only one pairbot satisfying a rule (rule 1). Therefore, even under an ASYNC scheduler, only one pairbot can move. After one step, another configuration appears; however, in this configuration, only one pairbot satisfies a rule (rule 2). In all subsequent configurations, only one pairbot can move. After 8 steps, a configuration that is a translation of the configuration C_{init} appears, which means that all robots move to the adjacent point at the same direction. Figure 10 shows the robot that satisfies a rule (a white robot), and the rule number can be applied in each configuration.*

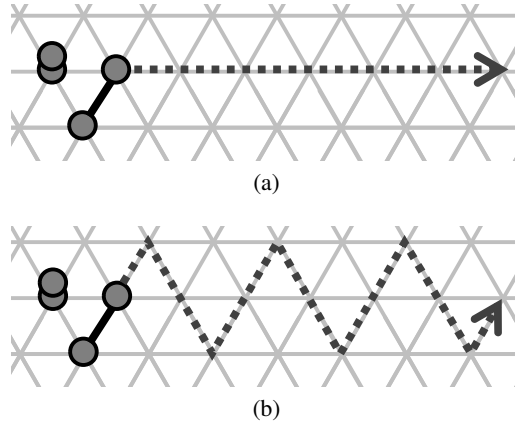


Figure 7: Examples of feasible perpetual marching

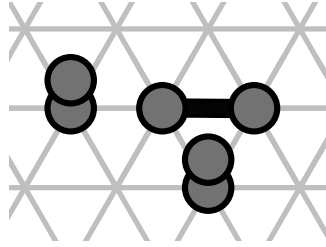
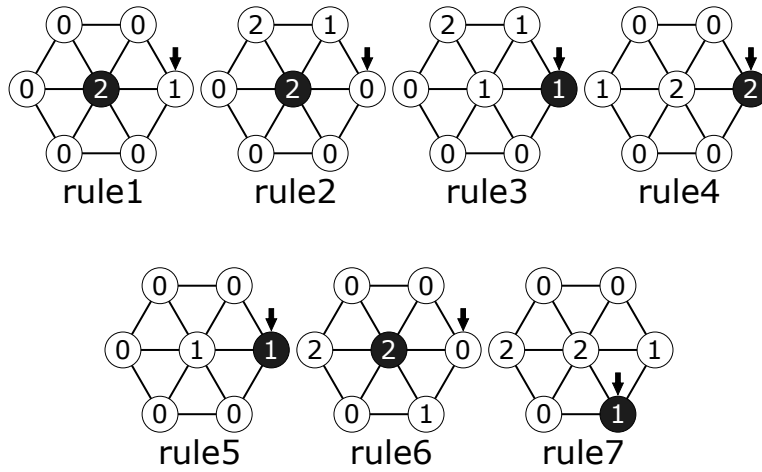
Figure 8: An well-initiated Configuration C_{init} 

Figure 9: The proposed algorithm for perpetual marching

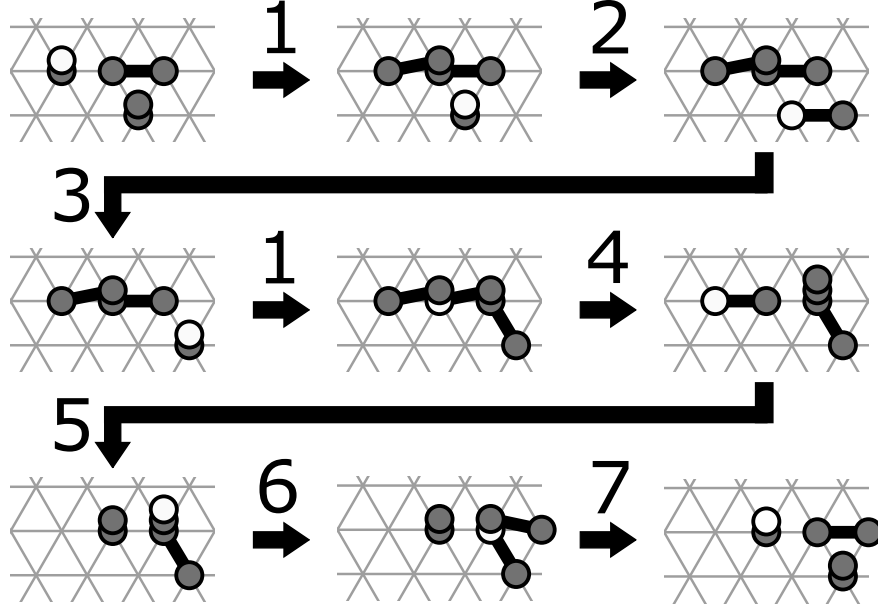


Figure 10: Execution of the proposed algorithm

As a result, in every configuration, the proposed algorithm moves only one robot, and eight different configurations sequentially appear while moving one hop in a certain direction. This implies that the proposed algorithm solves the perpetual marching problem.

By the proof of Lemma 1, the following corollary holds.

Corollary 1 *The proposed algorithm moves all the robots to a predetermined direction (by an initial configuration) with a distance of 1 in 8 steps.*

Here the term *steps* means the total number of robots that moves. By Lemma 1 and Corollary 1, the following theorem holds.

Theorem 1 *When a well-initiated configuration is given, the proposed algorithm solves the perpetual marching problem by moving all the robots to the same direction with a distance of 1 in every 8 steps under an ASYNC scheduler.*

Note that the proposed algorithm is optimal in terms of the number of *pairbots*; impossibility results for 1 *pairbot* or 2 *pairbots* can be easily proven because the total number of (feasible) configurations is small enough.

3.3 Pseudocode of the Perpetual Marching Algorithm

In this section, we present the pseudocode of the proposed algorithm to solve the perpetual marching by *pairbots* without a sense of direction.

Algorithm 1 shows the proposed algorithm. The proposed algorithm consists of 7 rules; each rule is presented as [Rule No.]: [Condition] \rightarrow [Action], which means that a robot executes an [Action] when [Condition] in the same [Rule No.] is satisfied. Since robots do not agree on any axis nor chirality, all conditions in the algorithm are **rotatable** and **reflectable**; which means that the condition for each rule becomes TRUE if the observed result of the robot satisfies the condition when rotated and/or mirrored in any direction.

3.4 Impossibility Result of Perpetual Marching by LCM-Robots

Now we discuss the *perpetual marching* problem also in *LCM* model, with no geometric agreement (i.e., without a sense of directions). If we assume an FSYNC scheduler, the problem can be easily solved by 3 autonomous mobile robots with visibility range 1 using the following algorithm.

- Initial configuration C_{init} : Let u and v be the two adjacent points. The robot r_1 is located u and the robots r_2 and r_3 are located v .

Algorithm 1 Algorithm for perpetual marching**variables and functions:**

- $\text{Buddy} \in \{\ell_0, \ell_1, \dots, \ell_6\}$: A label where its *buddy* exists.
- $\text{Chk}(\ell_x, \text{Nr})$: A function for checking the number of robots that returns TRUE when the number of robots on the adjacent point at ℓ_x is the same as Nr. Note that $\text{Nr} \in \{0, 1, 2\}$ due to weak multiplicity detection. The first parameter can be a set of labels $\mathbf{L} \subseteq \{\ell_x | 0 \leq x \leq 6\}$; the function returns TRUE only when $\text{Chk}(\forall \ell_x \in \mathbf{L}, \text{Nr}) = \text{TRUE}$.
- $\text{Move}(\ell_x)$: Move to ℓ_x .

algorithm:

```

/* All conditions are rotatable and reflectable:
   the condition for each rule becomes TRUE if the observed result of the robot satisfies
   the condition when rotated and/or mirrored in any direction.*/
Rule1: Buddy =  $\ell_0 \wedge \text{Chk}(\{\ell_2, \ell_3, \ell_4, \ell_5, \ell_6\}, 0) \wedge \text{Chk}(\ell_1, 1) \rightarrow \text{Move}(\ell_1)$ 
Rule2: Buddy =  $\ell_0 \wedge \text{Chk}(\{\ell_1, \ell_2, \ell_3, \ell_4\}, 0) \wedge \text{Chk}(\ell_5, 2) \wedge \text{Chk}(\ell_6, 1) \rightarrow \text{Move}(\ell_1)$ 
Rule3: Buddy =  $\ell_1 \wedge \text{Chk}(\{\ell_2, \ell_3, \ell_4\}, 0) \wedge \text{Chk}(\{\ell_0, \ell_1, \ell_6\}, 1) \wedge \text{Chk}(\ell_5, 2) \rightarrow \text{Move}(\ell_1)$ 
Rule4: Buddy =  $\ell_0 \wedge \text{Chk}(\{\ell_2, \ell_3, \ell_5, \ell_6\}, 0) \wedge \text{Chk}(\ell_1, 2) \wedge \text{Chk}(\ell_4, 1) \rightarrow \text{Move}(\ell_1)$ 
Rule5: Buddy =  $\ell_1 \wedge \text{Chk}(\{\ell_2, \ell_3, \ell_4, \ell_5, \ell_6\}, 0) \wedge \text{Chk}(\{\ell_0, \ell_1\}, 1) \rightarrow \text{Move}(\ell_1)$ 
Rule6: Buddy =  $\ell_0 \wedge \text{Chk}(\{\ell_1, \ell_3, \ell_5, \ell_6\}, 0) \wedge \text{Chk}(\ell_2, 1) \wedge \text{Chk}(\ell_4, 2) \rightarrow \text{Move}(\ell_1)$ 
Rule7: Buddy =  $\ell_0 \wedge \text{Chk}(\{\ell_3, \ell_5, \ell_6\}, 0) \wedge \text{Chk}(\ell_2, 1) \wedge \text{Chk}(\ell_4, 2) \rightarrow \text{Move}(\ell_2)$ 

```

- Algorithm: If a single robot observes two accompanied robots, it moves to the point occupied by them. If an accompanied robot observes a single robot, it moves to the point opposite to it.

Two pivotal questions naturally emerge:

1. "Is the perpetual marching problem solvable by LCM-robots under either an SSYNC or an ASYNC scheduler?"
2. "What is the minimum number of LCM-robots required to solve the perpetual marching problem in the LCM model under either an SSYNC or an ASYNC scheduler?"

To partially address these queries, we show the following theorem in this section.

Theorem 2 *Under an SSYNC scheduler, no deterministic algorithm exists that can solve the perpetual marching problem using unoriented (i.e., lacking geometric agreement) LCM-robots with a visibility range of 1, provided the number of robots is six or fewer.*

Now we prove Theorem 2 in the following subsections.

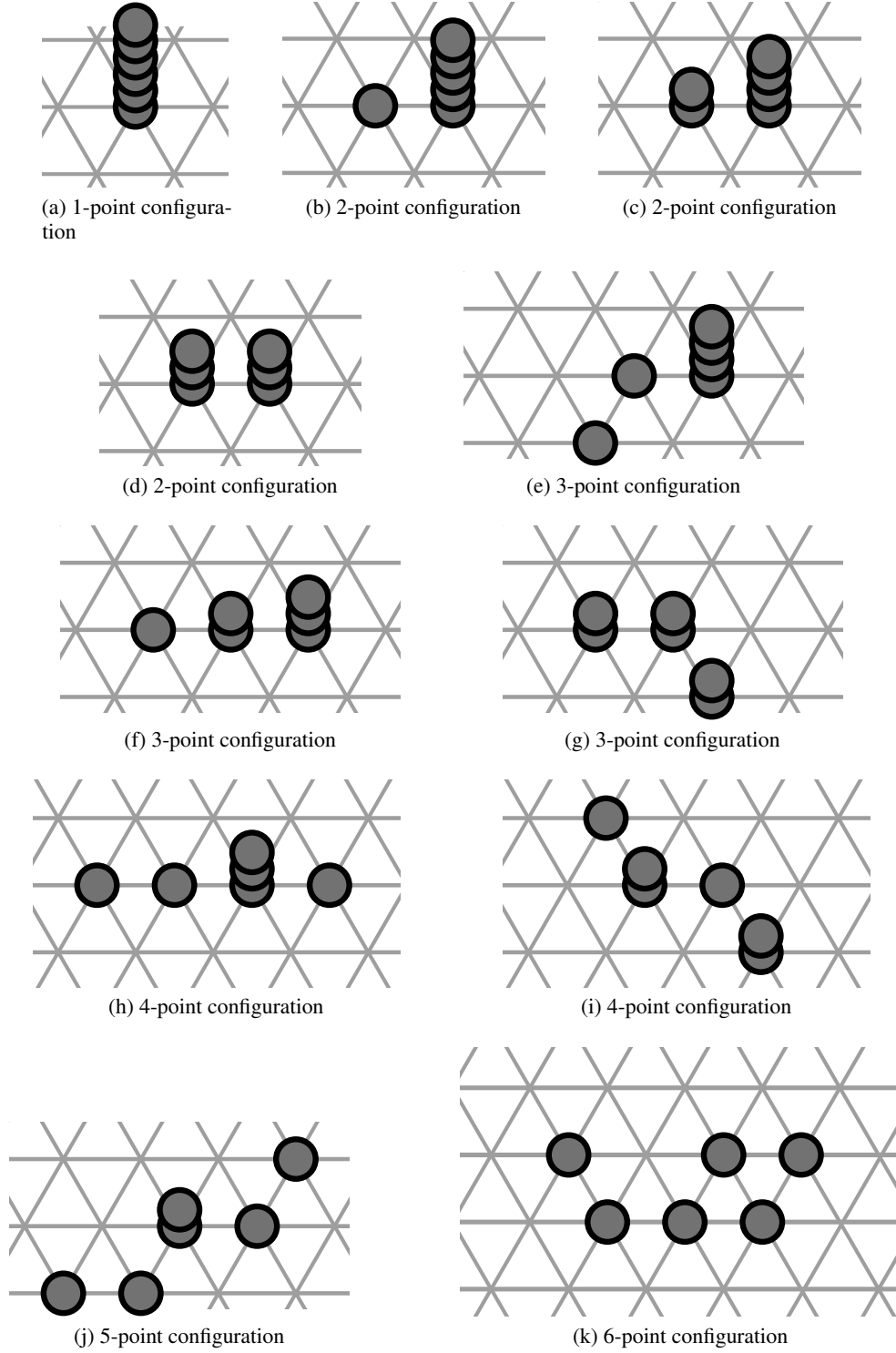
3.4.1 Preliminaries

Let $R = \{r_1, r_2, \dots, r_6\}$ be a set of 6 autonomous mobile robots with visibility range 1. The robots do not have any geometrical agreement (i.e., they do not agree on any axis nor chirality). Moreover, we assume that each robot has the capability of weak multiplicity detection. Here we consider an SSYNC scheduler.

A configuration C_i consists of all positions of all robots in R , and we call two configurations C_i and C_j is different when C_i cannot be transformed into C_j through translation, mirroring, and/or rotation. We consider a set of all *connected* configurations consisting of 6 autonomous mobile robots $\mathbb{C} = \{C_1, C_2, C_3, \dots, C_n\}$ such that configurations c_i and c_j for any i and j ($i \neq j$) are different configurations. A configuration C_i is a k -point configuration if exactly k points are occupied in C_i . Let \mathbb{C}^k be a set of all k -point configuration in \mathbb{C} ; $\mathbb{C}^1 \cup \mathbb{C}^2 \cup \mathbb{C}^3 \cup \mathbb{C}^4 \cup \mathbb{C}^5 \cup \mathbb{C}^6 = \mathbb{C}$ and $\mathbb{C}^1 \cap \mathbb{C}^2 \cap \mathbb{C}^3 \cap \mathbb{C}^4 \cap \mathbb{C}^5 \cap \mathbb{C}^6 = \emptyset$. Figure 11 shows the examples of k -point configurations by 6 robots.

Algorithm \mathcal{A} consists of a set of rules; a rule Rule_i is defined as a tuple $(\text{View}_i, \text{Dest}_i)$ which means that a robot moves to Dest_i if its observation result is the same as View_i . Note that the number of the possible observation results is finite (because the visibility range is assumed to 1), the number of the possible actions is also finite (because each robot can move to a point among its 6 adjacent points). Let $\mathcal{R} = \{\text{Rule}_1, \text{Rule}_2, \dots, \text{Rule}_m\}$ be a set of all possible rules. Algorithm \mathcal{A} can be defined as a set of (non-conflicted) rules $\mathcal{R}_{\mathcal{A}} \subset \mathcal{R}$.

Now we consider an algorithm-based directed graph $\overrightarrow{G_{\mathcal{A}}} = (V, A_{\mathcal{A}})$ where $V = \mathbb{C} \cup \{C_{\text{disCon}}\}$. Arc (i.e., directed edge) $(C_i, C_j) \in E_{\mathcal{A}}$ if C_j is obtained when a robot performs its *Move* operation according to a rule in algorithm

Figure 11: Examples of k -point configurations

\mathcal{A} in configuration C_i ; $C_i \mapsto_{(r_k, \mathcal{A})} C_j$ where robot r_k satisfies a rule in \mathcal{A} . Moreover, arc (i.e., directed edge) $(C_i, C_{disCon}) \in E_{\mathcal{A}}$ if a non-connected configuration is obtained when a robot executes a rule in \mathcal{A} in configuration C_i .

3.4.2 Basic Strategy of the Proof

First, we present the basic strategy of the proof. We assume an SSYNC scheduler, this means that in each round, the scheduler determines a set of robots and they executes the (same) algorithm. If there exists an algorithm to solve the perpetual marching problem, it must be able to handle all patterns from all possible schedulers. Additionally, since the robots do not have a sense of direction, the destination point a robot moves to may not be uniquely determined depending on the rule in the algorithm. An algorithm for the perpetual marching problem must work correctly even when the destination is arbitrarily selected. Therefore, in the proof of impossibility, we assume that both the scheduler and the destination are chosen adversarially, and show that there is no algorithm can solve the perpetual marching problem.

In the proof of impossibility, we assume the following adversarial scenarios:

1. When there are two robots satisfying $View_i$ and if they simultaneously execution of $Rule_i$ makes the perpetual marching impossible, the scheduler selects these two robots and makes them act in a way that makes the perpetual marching impossible.
2. Except for **1**, the scheduler always selects only one point where there exists a robot satisfies any rule in the algorithm, and make all the robots at the point simultaneously execute the algorithm (i.e., the scheduler never selects two different robots at two different points).
3. In the case of **2**, when the destination is arbitrarily selected, all robots choose the same direction. In other words, if multiple robots are on the same point, they always move as a group and never scatter during execution.
4. If a destination is not uniquely determined by a rule, the scheduler selects destinations in a way that results in unfavorable configuration transitions (e.g., if a specific movement of some robots causes a disconnected configuration, the scheduler selects that destination).

We generate digraph $\overrightarrow{G_{\mathcal{A}}}$ as a configuration transition diagram under the above scenario to prove the impossibility. If there is algorithm \mathcal{A} to solve the perpetual marching problem, digraph $\overrightarrow{G_{\mathcal{A}}}$ includes a directed cycle (denote $\vec{\mathcal{C}}_f = (C_i, C_j, C_k, \dots, C_i)$) presenting an infinite execution (i.e., infinite transition of configurations) of algorithm \mathcal{A} .

Remind that every robot's visibility range is 1 and the robots do not agree on any axis nor chirality, thus a connected configuration cannot be obtained from any disconnected configuration due to an adversarial scheduler. Therefore, the following corollary holds.

Corollary 2 *If there exists directed cycle $\vec{\mathcal{C}}_f$ in digraph $\overrightarrow{G_{\mathcal{A}}}$, $\vec{\mathcal{C}}_f$ consists of only connected configurations.*

We call an infinite execution of algorithm \mathcal{A} from an well-initiated configuration (i.e., any configuration appeared in $\vec{\mathcal{C}}_f$) the execution of $\vec{\mathcal{C}}_f$.

Moreover, we call directed cycle $\vec{\mathcal{C}}_f$ in digraph $\overrightarrow{G_{\mathcal{A}}}$ is *illegible*, if $\vec{\mathcal{C}}_f$ satisfies any of the following conditions.

1. **(No movement)** Let C_i be a well-initiated configuration in $\vec{\mathcal{C}}_f$. After the constant number of executions, when C_i appears again (denote as C_i^2), all the robots are at the exactly same points in C_i and C_i^2 .
2. **(Faulty concurrency)** In configuration C_i in $\vec{\mathcal{C}}_f$, there are two different robots (r_x and r_y) and two different rules ($Rule_x$ and $Rule_y$ in \mathcal{A}) such that robot r_x (resp. r_y) can execute $Rule_x$ (resp. $Rule_y$). When the two robots simultaneously execute \mathcal{A} , configuration C_j which is not included in $\vec{\mathcal{C}}_f$ is obtained.
3. **(Adversarial transition)** Let C_i be a configuration in $\vec{\mathcal{C}}_f$, and C_j be a configuration NOT in $\vec{\mathcal{C}}_f$. There exists arc (C_i, C_j) in $A_{\mathcal{A}}$.

3.4.3 Proof of Impossibility Result

Let \mathcal{A} be an algorithm to solve the perpetual marching problem by autonomous mobile robots with visibility range 1 under an SSYNC scheduler.

We call a rule such that when a robot executes the rule, all the robots located at seven points within the visibility range of the robot become disconnected a *locally disconnecting rule*.

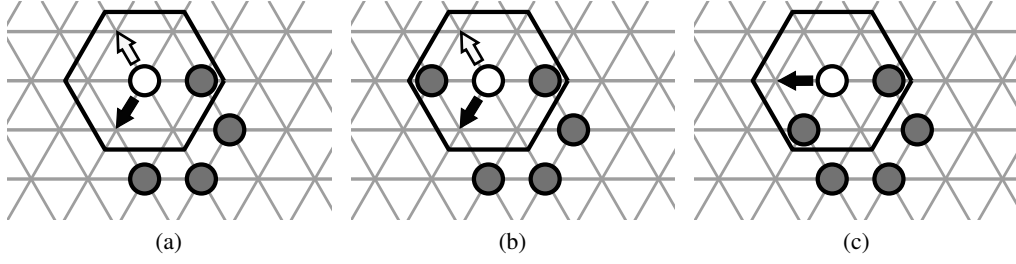


Figure 12: Examples of locally disconnecting rules

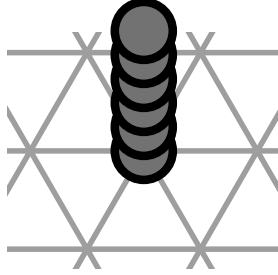
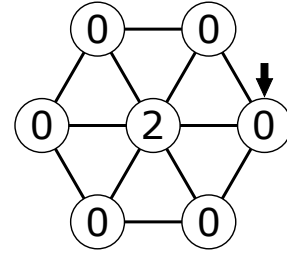
Figure 13: Unique configuration C_1^1 in \mathbb{C}^1 Figure 14: Only one feasible rule in C_1^1

Figure 12 shows some examples of locally disconnecting rules. In each figure, a hexagon represents a local view of the observing robot (white circle) and each arrow shows a destination to move when the robot obtains such an observation result. Depending on the configuration, even if some rule (e.g., Figure 12(c)) is executed, there are cases where the next configuration remains connected. However, in some configurations, it is possible for it to become disconnected. Since the robots executing the rules cannot perceive configurations outside their visibility range, adding locally disconnecting rules to the algorithm \mathcal{A} may result in execution even in cases where it becomes disconnected, leading to disconnected configurations. From the above fact and Corollary 2, the following lemma holds.

Lemma 2 *There is no locally disconnecting rule in algorithm \mathcal{A} .*

Now we have prepared the groundwork to proceed with the proof of impossibility. We show the impossibility by showing that none of the vertices in the graph are included in $\vec{\mathcal{C}}_f$. Specifically, we start by proving that none of the points in all 1-point configurations ($\in \mathbb{C}^1$) are included, and then consider the points in all 2-point configurations (\mathbb{C}^2). In any 2-point configuration, we utilize the fact that the algorithm does not contain rules that transform the configuration into any 1-point configuration to reduce the number of vertices to consider. This is achieved by ensuring that when two robots at different points move to the same point once, the scheduler always activates these two robots simultaneously, providing the same view and ensuring that they always perform the same operations (remind that we consider a deterministic algorithm). This implies that if configuration C_i in \mathbb{C}^k is obtained from configuration C_j ($i \neq j$) in $\mathbb{C}^{(k+1)}$ by an algorithm, configuration C_i cannot be obtained again by the algorithm due to an adversarial scheduler. Hence the following corollary holds.

Corollary 3 *If there exists directed cycle $\vec{\mathcal{C}}_f$ (i.e., algorithm to solve the perpetual marching exists), all the configurations included in $\vec{\mathcal{C}}_f$ are the same k -point configurations (i.e., $\forall C_i, C_j \in \vec{\mathcal{C}}_f : \{C_i, C_j\} \subseteq \mathbb{C}^k$).*

From the definition of k -point configuration, there is only one configuration included in \mathbb{C}^1 . Figure 13 presents the unique configuration of 1-point configuration (\mathbb{C}^1).

Lemma 3 *Let C_1^1 be the unique configuration in \mathbb{C}^1 . Cycle $\vec{\mathcal{C}}_f$ never includes C_1^1 .*

Proof 2 *Configuration C_1^1 is the same as the configuration depicted in Figure 11(a). This implies that all the robots have the same observation result. Figure 14 represents the observation result of every robot in C_1^1 (the notation of the rule is the same as the graphical representation of the algorithm for perpetual marching; refer to Section 3.2). The destination of the rule presented in Figure 14 is the point on the right, however, the destination point is irrelevant in this*

rule. In other words, this means that the rule remains the same regardless of where the destination point is because the robots do not agree any axis. We call this rule Rule₁.

Assume that configuration C_1^1 is included in $\vec{\mathcal{C}}_f$. If algorithm \mathcal{A} includes Rule₁, the scheduler activates all the 6 robots simultaneously, and makes them to move to the same point. After that, the scheduler activates all the robots again, and makes them to return back to the previously located point. By repeating this, no robot cannot move to any other point than these two points. As a result, the perpetual marching cannot be solved. If algorithm \mathcal{A} does not include Rule₁, no robot cannot move. Therefore, there is no algorithm to solve the perpetual marching problem from configuration C_1^1 , and this implies that configuration C_1^1 is not included in $\vec{\mathcal{C}}_f$.

Lemma 4 Cycle $\vec{\mathcal{C}}_f$ never includes any configuration in \mathbb{C}^2 .

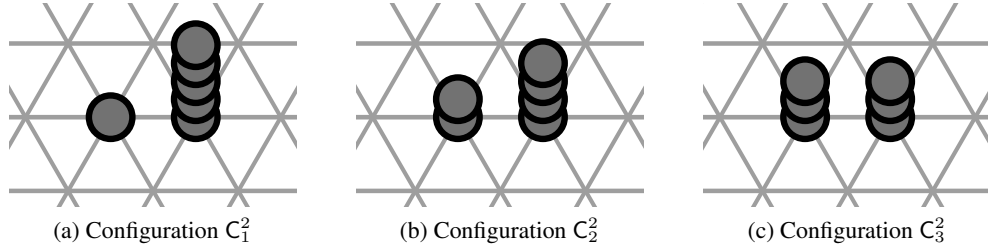


Figure 15: Three configurations in \mathbb{C}^2

Proof 3 Figure 15 shows all the 2-point configurations (\mathbb{C}^2). Note that all the robots in any of two configuration C_2^2 and C_3^2 have the same observation results due to the weak multiplicity.

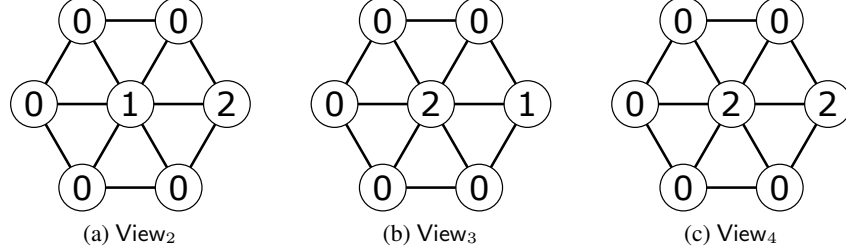


Figure 16: Three views of the robots in \mathbb{C}^2

Figure 16 presents the view can be observed by the robots in 2-point configuration (we call these three views View₂, View₃, and View₄ respectively). In any configuration in \mathbb{C}^2 , each robot obtains one of the observation result among View₂, View₃ and View₄. By Lemma 2, considering any locally disconnecting rule is not required, thus only the three rules depicted in Figure 17 have to be considered.

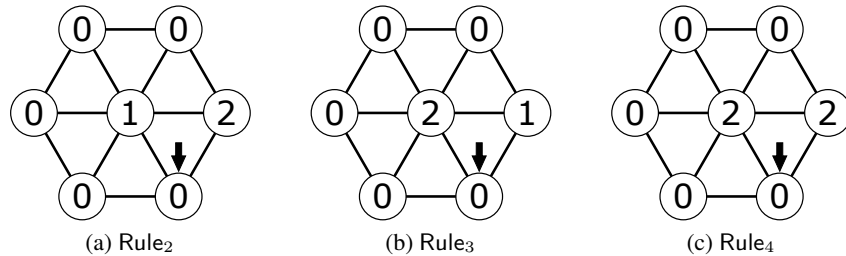
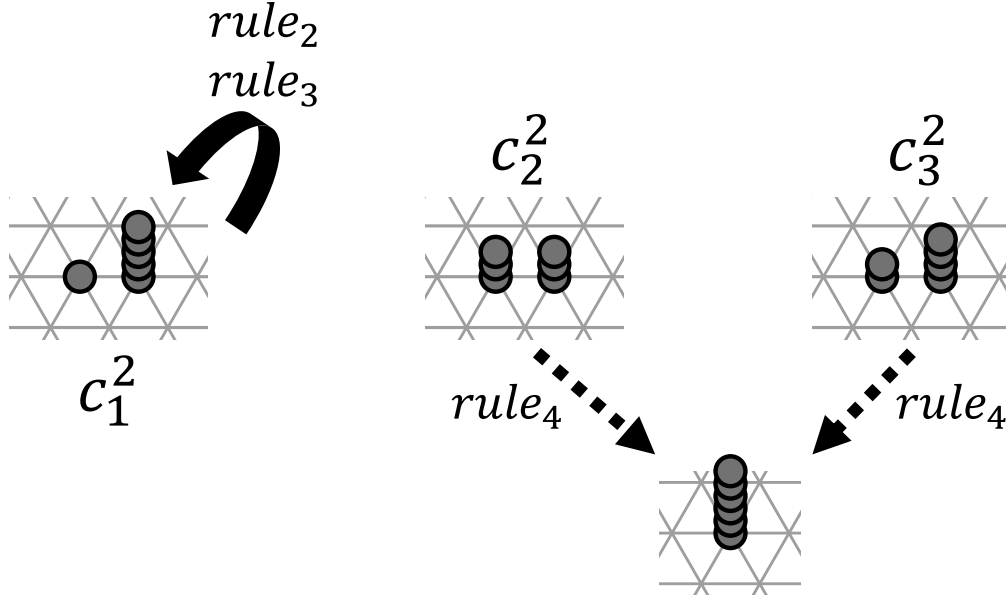


Figure 17: Three feasible rules in \mathbb{C}^2

Figure 18: Configuration transition in \mathbb{C}^2

Assume that configuration \mathbb{C}_1^2 is included in $\vec{\mathcal{C}}_f$. If algorithm \mathcal{A} includes Rule₂ (resp. Rule₃), the scheduler activates a single robot (resp. all 5 robots located at the same point). And the same configuration (\mathbb{C}_1^2) appears again (refer to Figure 18). In the next activation, the scheduler can make the single robot (or the 5 robots) to move back to the previously occupying point. Thus configuration \mathbb{C}_1^2 is not included in $\vec{\mathcal{C}}_f$.

Now assume that configuration \mathbb{C}_2^2 and/or \mathbb{C}_3^2 is included in $\vec{\mathcal{C}}_f$. In this case, only View₄ can be obtained by the robots. If algorithm \mathcal{A} includes Rule₄, the scheduler can activate all the 6 robots, and make them to move to the same point causing 1-point configuration by faulty concurrency. Therefore, configurations \mathbb{C}_2^2 and \mathbb{C}_3^2 are not included in $\vec{\mathcal{C}}_f$.

Lemma 5 Cycle $\vec{\mathcal{C}}_f$ never includes any configuration in \mathbb{C}^3 .

Proof 4 First, we present all the configurations included in \mathbb{C}^3 as Figure 19. There are 15 3-point configurations, we denote the configurations by \mathbb{C}_1^3 to \mathbb{C}_{15}^3 , $\mathbb{C}^3 = \{\mathbb{C}_1^3, \mathbb{C}_2^3, \dots, \mathbb{C}_{15}^3\}$.

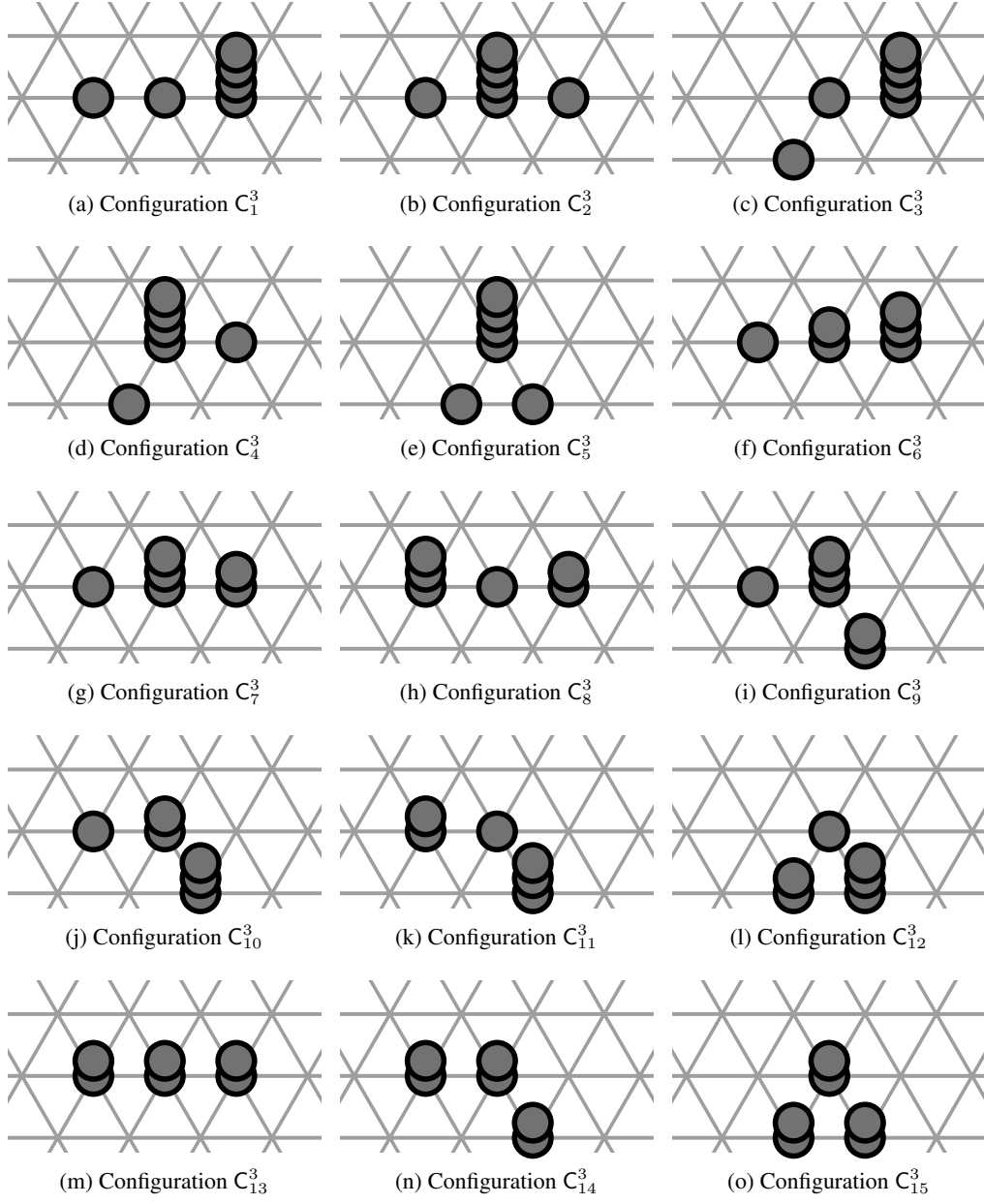
From configurations \mathbb{C}_1^3 to \mathbb{C}_{15}^3 , we can enumerate all the views can be obtained by any robots in \mathbb{C}^3 . Figure 16 shows all the views in any configuration in \mathbb{C}^3 (19 views exist). Note that views View₂, View₃, and View₄ are the same as them appeared in \mathbb{C}^2 .

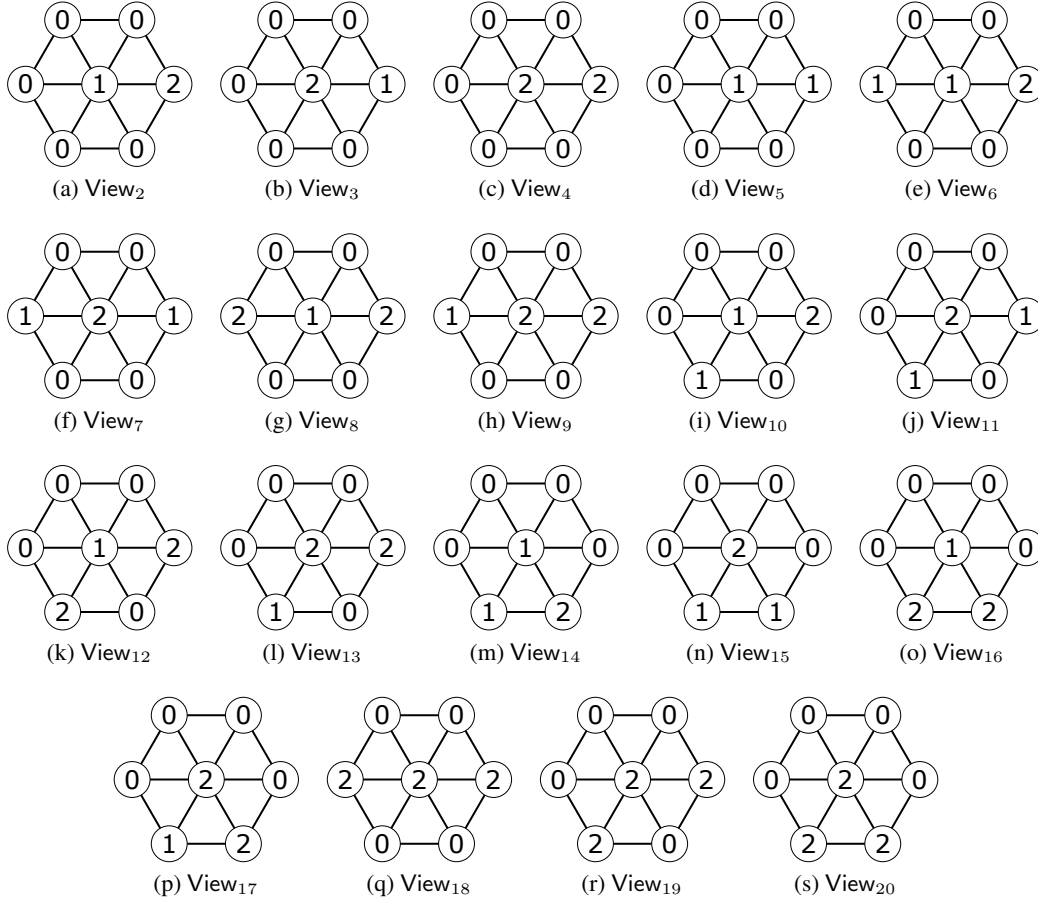
From all the views obtained by a robot in any configuration in \mathbb{C}^3 , we can enumerate all feasible rules. Also in this case, we do not consider a locally disconnecting rule (due to Lemma 2). Moreover, we also exclude a rule that makes a robot to any point occupied by another robot because such a rule causes a configuration in \mathbb{C}^1 or \mathbb{C}^2 (refer to Corollary 3). As a result, we obtain the 16 rules depicted in Figure 21.

Now we can obtain the induced subgraph $\overrightarrow{G_{Al}}(\mathbb{C}^3)$ of $\overrightarrow{G_{Al}}$ because the set of arcs in $\overrightarrow{G_{Al}}(\mathbb{C}^3)$ is defined by the rules in Figure 21. It is worthwhile to mention that no robot can distinguish the difference between \mathbb{C}_6^3 and \mathbb{C}_7^3 , and between \mathbb{C}_9^3 and \mathbb{C}_{10}^3 due to the weak multiplicity.

Figure 22 presents the induced subgraph $\overrightarrow{G_{Al}}(\mathbb{C}^3)$. A dotted arc represents an execution occurring a disconnected configuration or a smaller k -point configuration due to a faulty concurrency. There are 6 (directed) loops at configurations \mathbb{C}_3^3 , \mathbb{C}_4^3 , \mathbb{C}_9^3 , \mathbb{C}_{10}^3 , \mathbb{C}_{11}^3 , and \mathbb{C}_{14}^3 . An infinity execution of these loops are the same; only the robots located at the center point repeatedly move back and forth between two points. Thus these loops cannot become cycle $\vec{\mathcal{C}}_f$.

Now we consider the following two (directed) cycles, $(\mathbb{C}_1^3 \rightarrow \mathbb{C}_3^3 \rightarrow \mathbb{C}_1^3)$ and $(\mathbb{C}_6^3 \rightarrow \mathbb{C}_{10}^3 \rightarrow \mathbb{C}_6^3)$, and $(\mathbb{C}_7^3 \rightarrow \mathbb{C}_9^3 \rightarrow \mathbb{C}_7^3)$. However in any cycles, only some robots at the same point infinitely move back and forth between two adjacent points. This implies that there exists a robot which never moves, hence, these cycles cannot become cycle $\vec{\mathcal{C}}_f$.

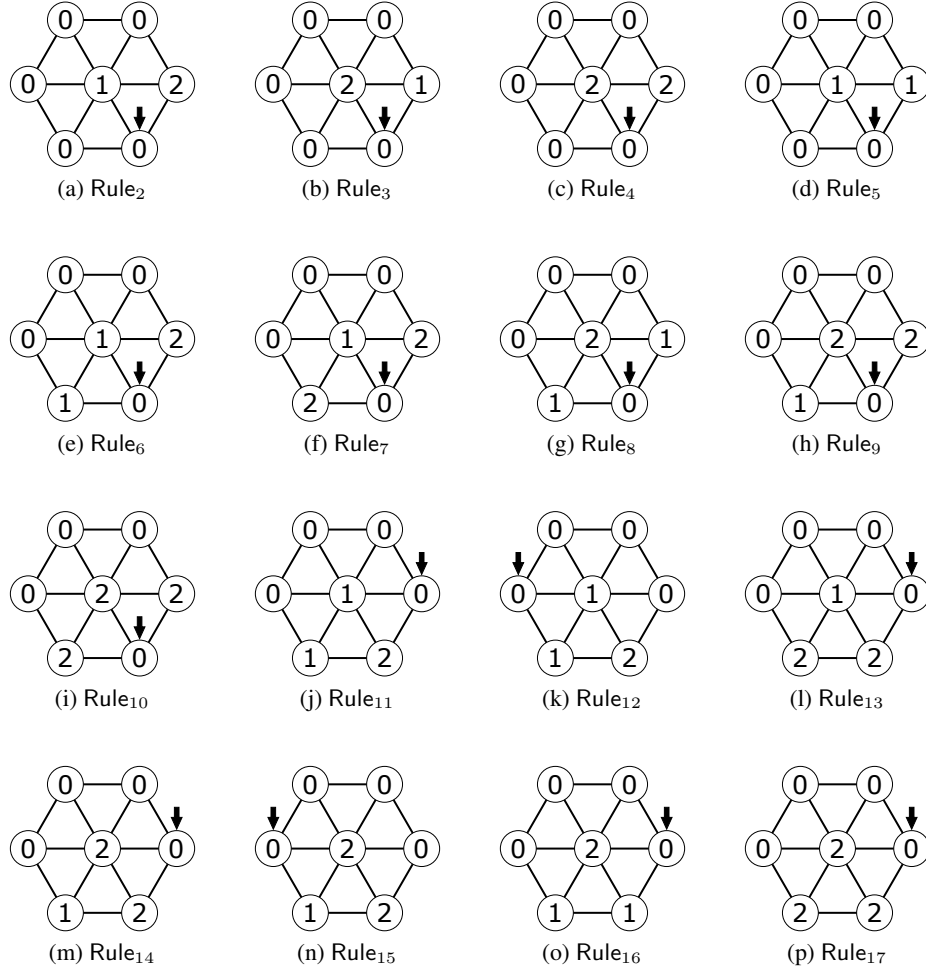
Figure 19: All the configurations in \mathbb{C}^3

Figure 20: All views can be obtained by a robot in \mathbb{C}^3

We can prove the remaining parts of the proof below using the same manner, but each proof becomes much more longer, thus we omit the detailed proofs of the following three lemmas for \mathbb{C}^4 , \mathbb{C}^5 , and \mathbb{C}^6 respectively here.

Lemma 6 Cycle $\vec{\mathcal{C}}_f$ never includes any configuration in \mathbb{C}^4 .

Proof 5 (Sketch) There are 47 configurations in \mathbb{C}^4 , and 40 views can be obtained by a robot in any configuration in \mathbb{C}^4 . From these views, we can obtain 36 feasible rules in \mathbb{C}^4 . A resultant induced subgraph $\vec{G}_{Al}(\mathbb{C}^4)$ of \vec{G}_{Al} is given in Figures 23 and 24. There are many cycles in $\vec{G}_{Al}(\mathbb{C}^4)$, however, no appropriate cycle in $\vec{G}_{Al}(\mathbb{C}^4)$ which can become feasible $\vec{\mathcal{C}}_f$.

Figure 21: All feasible rules in \mathbb{C}^3

Lemma 7 Cycle $\vec{\mathcal{C}}_f$ never includes any configuration in \mathbb{C}^5 .

Lemma 8 Cycle $\vec{\mathcal{C}}_f$ never includes any configuration in \mathbb{C}^6 .

We omit the proof of Lemmas 7 and 8 however these can be proven by the same manner; there exist 87 and 82 configurations in $\vec{G}_{AI}(\mathbb{C}^5)$ and $\vec{G}_{AI}(\mathbb{C}^6)$ respectively.

From lemmas 3, 4, 5, 6, 7, and 8, the following lemma holds.

Lemma 9 There is no directed cycle $\vec{\mathcal{C}}_f$ in $\vec{G}_{\mathcal{A}} = (G, A_{\mathcal{A}})$ implying the valid infinite execution of the perpetual marching.

Therefore, the following theorem holds by Lemma 9.

Theorem 3 Under an SSYNC scheduler, no deterministic algorithm exists that can solve the perpetual marching problem using unoriented (i.e., lacking geometric agreement) LCM-robots with a visibility range of 1, provided the number of robots is six.

Theorem 3 presents an impossibility result only for 6 LCM-robots, however, an impossibility result for 5 or less LCM-robots can be easily proven. In particular, the impossibility results for 1, 2, or 3 LCM-robots can be proven by a straight-forward manner (only the small number of all connected configurations exist), and the results for 4 or 5

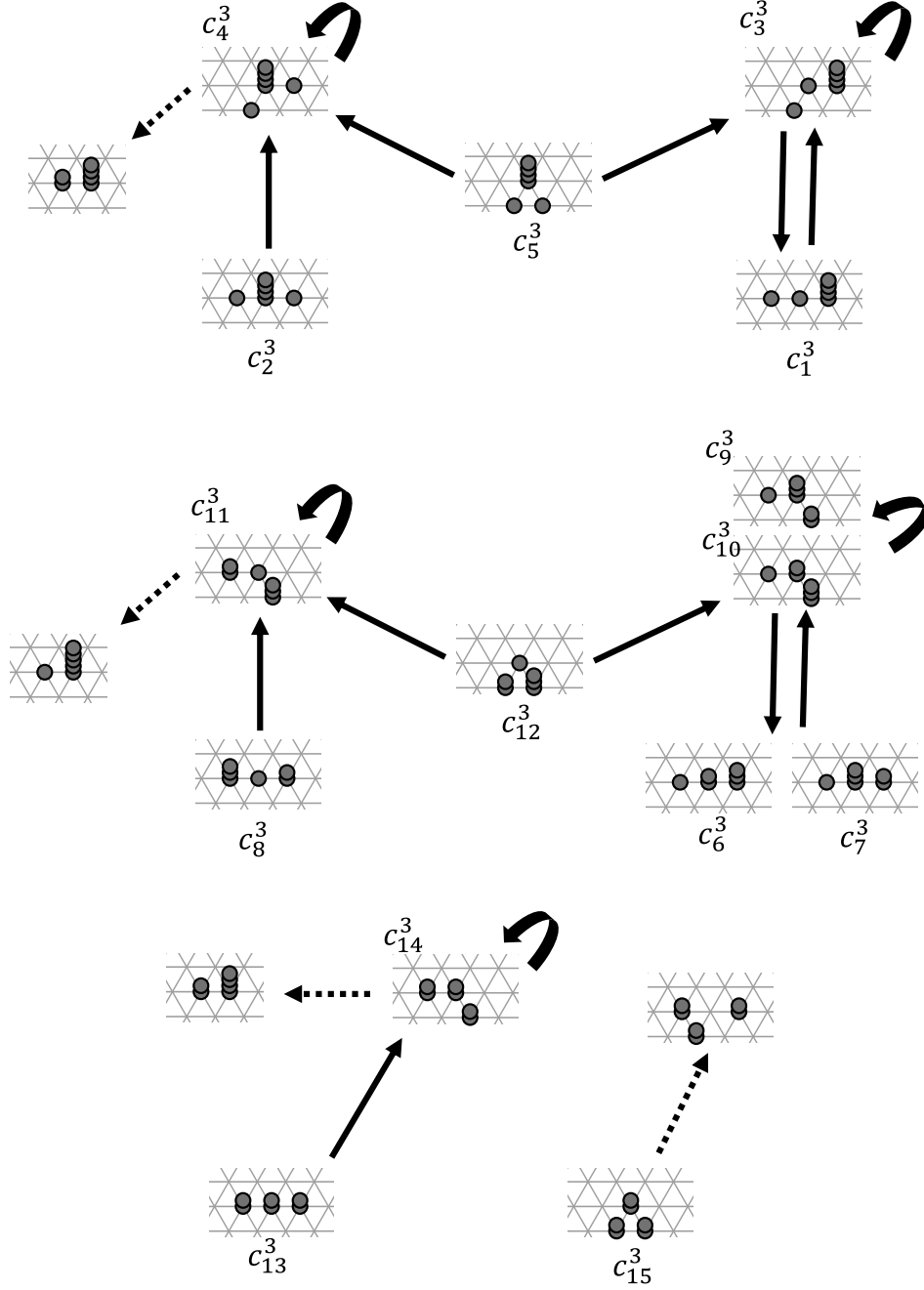


Figure 22: Configuration transition in \mathbb{C}^3 (i.e., the induced subgraph $\overrightarrow{G_{AI}}(\mathbb{C}^3)$ of $\overrightarrow{G_{AI}}$)

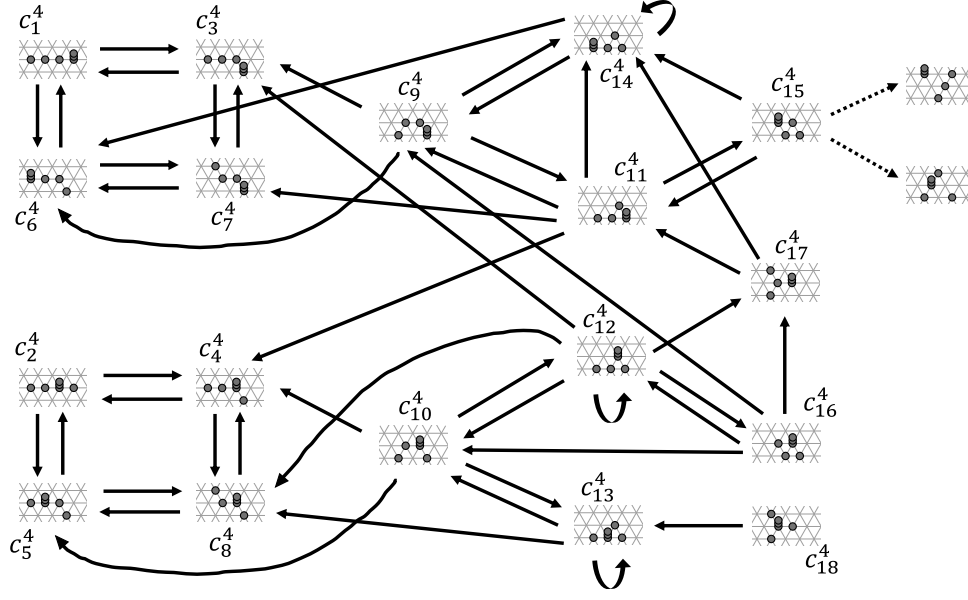


Figure 23: Configuration transition in \mathbb{C}^4 (i.e., the induced subgraph $\overrightarrow{G_{Al}}(\mathbb{C}^4)$ of $\overrightarrow{G_{Al}}$): From C_1^4 to C_{18}^4

LCM-robots can be proven as the same manner as the case for 6 LCM-robots. However, many of k -point configurations appeared when the number of robots is 4 or 5 are also appeared in the proof for 6 LCM-robots, thus, there are only some configurations have to be newly considered to prove the impossibility result. As a result, Theorem 2 holds.

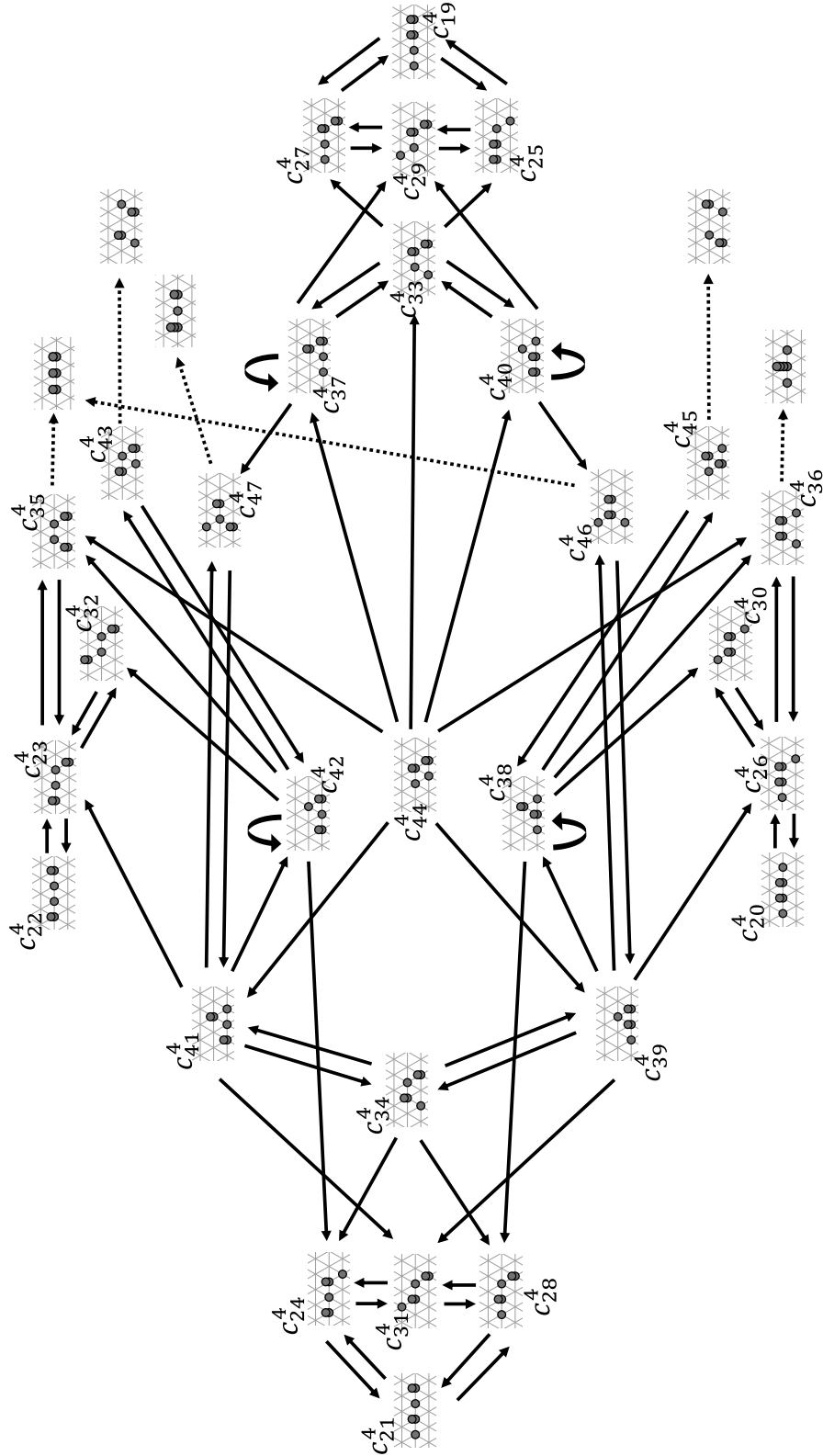


Figure 24: Configuration transition in \mathbb{C}^4 (i.e., the induced subgraph $\vec{G}_{AI}(\mathbb{C}^4)$ of \vec{G}_A): From C_{19}^4 to C_{47}^4

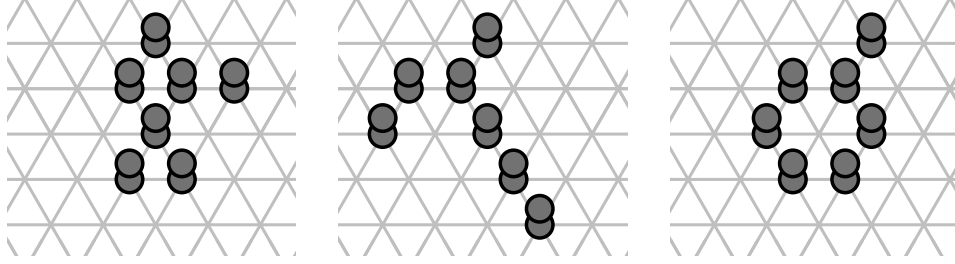


Figure 25: Examples of initial configurations

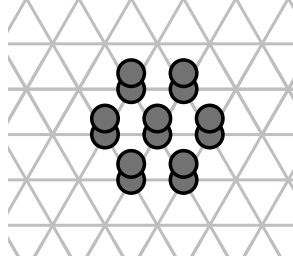


Figure 26: Goal configuration

4 The 7-pairbots-gathering Problem

4.1 Problem Definition

In this section, we consider the 7-pairbots-gathering problem, which is the gathering problem of 7 *pairbots* on a triangular grid. Generally, many gathering problems aim to gather all robots to one common point, but here we consider the gathering problem where two or more robots do not exist at the same point like the gathering considered in fat robot models Czyzowicz et al. [2009]. This means that our goal is to gather the robots as close together as possible.

We define the 7-*pairbots*-gathering problem as the following.

Definition 2 7-pairbots-gathering Problem. *Given an arbitrary connected configuration consisting of 7 pairbots in short state, algorithm \mathcal{A} solves the 7-pairbots-gathering problem if \mathcal{A} satisfies all the following conditions: (1) algorithm \mathcal{A} eventually terminates; algorithm \mathcal{A} eventually reaches a configuration such that no robot can move, (2) all pairbots are in short state and no two pairbots exist at the same point when algorithm \mathcal{A} terminates, and (3) $\text{dist}(r_i, r_j) \leq 2$ for any non-paired two robots r_i and r_j when algorithm \mathcal{A} terminates.*

Figure 25 shows three examples of initial configurations and Figure 26 illustrates the goal configuration of 7-pairbots-gathering problem. Note that only one configuration as Figure 26 is allowed as a goal configuration.

We can also consider the 7-*robots*-gathering problem which is the gathering by 7 LCM-robots (robots in LCM model) instead of *pairbots*. This problem is already introduced in Shibata et al. [2022], and the two following theorems hold by the literature.

Theorem 4 Shibata et al. [2022] *For robots with visibility range 1, there exists no deterministic algorithm to solve the 7-robots-gathering problem even under an FSYNC scheduler.*

Theorem 5 Shibata et al. [2022] *For robots with visibility range 2, there exists a deterministic algorithm to solve the 7-robots-gathering problem from any connected initial configuration under an FSYNC scheduler.*

Theorems 4 and 5 suggest that the visibility range plays a critical role in the solvability of the 7-robots-gathering problem, especially under deterministic algorithms and an FSYNC scheduler. While it is unsolvable for robots with a visibility range of 1, the problem becomes solvable for robots with a visibility range of 2 if they start from any connected initial configuration. In the following, we show that the 7-pairbots-gathering problem for *pairbots* is solvable even with visibility range 1.

4.2 7-pairbots-gathering Algorithm

Here we introduce the proposed algorithm to solve the 7-pairbots-gathering algorithm using graphical representation. The detailed pseudocode of the algorithm will be presented in the next section.

Figures 27 shows the proposed algorithm by *pairbots* with a common sense of directions. Each white circle shows a *pairbot* that executes the proposed algorithm, and each black circle represents the observed robots. Each cross mark means a point which is not occupied by any robot, a triangle presents a point occupied one or more robots (in rules 14, 16, 17, and 21), and an inverted (reversed) triangle represents a point occupied two robots or no robot (in rule 41). Some rules for a *pairbot* in *long* state marks a asterisk near the *pairbot*, which means the robot executes the rule even if there are some other robots at the same (i.e., center) point (in rules from 7 to 11, 20, and 21). If there is no any mark at the point, the algorithm does not care about the point.

4.3 Pseudocode of the 7-pairbots-gathering Algorithm

In this section, we present the pseudocode of the proposed algorithm to solve the 7-pairbots-gathering problem. We assume that all robots agree on the orientation and directions of both axes, which is the same assumption as the literature Shibata et al. [2022]; every robot labels the adjacent point located on its right side as ℓ_1 , and then labels the other adjacent points from ℓ_2 to ℓ_6 in clockwise order (refer to the labeling of robot r_i in Figure 2). The point where a robot currently exists is labeled by ℓ_0 . Algorithm 2 shows the proposed algorithm; as the same as the algorithm in the previous section, each rule is presented as [Rule No.]: [Condition] \rightarrow [Action].

Algorithm 2 Algorithm for 7-pairbots-gathering

variables and functions:

- Buddy $\in \{\ell_0, \ell_1, \dots, \ell_6\}$: A label where its *buddy* exists.
- $\text{Chk}(\ell_x, \text{Nr})$: A function for checking the number of robots that returns TRUE when the number of robots on the adjacent point at ℓ_x is the same as Nr. Note that $\text{Nr} \in \{0, 1, 2\}$ due to weak multiplicity detection. The first parameter can be a set of labels $\mathbf{L} \subseteq \{\ell_x | 0 \leq x \leq 6\}$; the function returns TRUE only when $\text{Chk}(\forall \ell_x \in \mathbf{L}, \text{Nr}) = \text{TRUE}$.
- $\text{Move}(\ell_x)$: Move to ℓ_x .

algorithm:

- Rule1: Buddy = $\ell_0 \wedge \text{Chk}(\{\ell_2, \ell_3, \ell_4, \ell_5, \ell_6\}, 0) \wedge \text{Chk}(\ell_1, 2) \rightarrow \text{Move}(\ell_2)$
 - Rule2: Buddy = $\ell_0 \wedge \text{Chk}(\{\ell_1, \ell_3, \ell_4, \ell_5, \ell_6\}, 0) \wedge \text{Chk}(\ell_2, 2) \rightarrow \text{Move}(\ell_3)$
 - Rule3: Buddy = $\ell_0 \wedge \text{Chk}(\{\ell_1, \ell_2, \ell_4, \ell_5, \ell_6\}, 0) \wedge \text{Chk}(\ell_3, 2) \rightarrow \text{Move}(\ell_4)$
 - Rule4: Buddy = $\ell_0 \wedge \text{Chk}(\{\ell_1, \ell_2, \ell_3, \ell_5, \ell_6\}, 0) \wedge \text{Chk}(\ell_4, 2) \rightarrow \text{Move}(\ell_5)$
 - Rule5: Buddy = $\ell_0 \wedge \text{Chk}(\{\ell_1, \ell_2, \ell_3, \ell_4, \ell_6\}, 0) \wedge \text{Chk}(\ell_5, 2) \rightarrow \text{Move}(\ell_6)$
 - Rule6: Buddy = $\ell_0 \wedge \text{Chk}(\{\ell_1, \ell_2, \ell_3, \ell_4, \ell_5\}, 0) \wedge \text{Chk}(\ell_6, 2) \rightarrow \text{Move}(\ell_1)$
 - Rule7: Buddy = $\ell_2 \wedge \text{Chk}(\{\ell_3, \ell_4, \ell_5, \ell_6\}, 0) \wedge \text{Chk}(\ell_2, 1) \wedge \text{Chk}(\ell_1, 2) \rightarrow \text{Move}(\ell_2)$
 - Rule8: Buddy = $\ell_3 \wedge \text{Chk}(\{\ell_1, \ell_4, \ell_5, \ell_6\}, 0) \wedge \text{Chk}(\ell_3, 1) \wedge \text{Chk}(\ell_2, 2) \rightarrow \text{Move}(\ell_3)$
 - Rule9: Buddy = $\ell_4 \wedge \text{Chk}(\{\ell_1, \ell_2, \ell_5, \ell_6\}, 0) \wedge \text{Chk}(\ell_4, 1) \wedge \text{Chk}(\ell_3, 2) \rightarrow \text{Move}(\ell_4)$
 - Rule10: Buddy = $\ell_5 \wedge \text{Chk}(\{\ell_1, \ell_2, \ell_6\}, 0) \wedge \text{Chk}(\ell_5, 1) \wedge \text{Chk}(\ell_4, 2) \rightarrow \text{Move}(\ell_5)$
 - Rule11: Buddy = $\ell_6 \wedge \text{Chk}(\{\ell_1, \ell_2, \ell_3, \ell_4\}, 0) \wedge \text{Chk}(\ell_6, 1) \wedge \text{Chk}(\ell_5, 2) \rightarrow \text{Move}(\ell_6)$
 - Rule12: Buddy = $\ell_1 \wedge \text{Chk}(\{\ell_2, \ell_3, \ell_4, \ell_5\}, 0) \wedge \text{Chk}(\{\ell_0, \ell_1\}, 1) \wedge \text{Chk}(\ell_6, 2) \rightarrow \text{Move}(\ell_1)$
 - Rule13: Buddy = $\ell_0 \wedge \text{Chk}(\{\ell_2, \ell_3, \ell_4, \ell_5\}, 0) \wedge \text{Chk}(\{\ell_1, \ell_6\}, 2) \rightarrow \text{Move}(\ell_2)$
 - Rule14: Buddy = $\ell_0 \wedge \text{Chk}(\{\ell_3, \ell_4, \ell_5, \ell_6\}, 0) \wedge \neg \text{Chk}(\ell_1, 0) \wedge \text{Chk}(\ell_2, 2) \rightarrow \text{Move}(\ell_3)$
 - Rule15: Buddy = $\ell_0 \wedge \text{Chk}(\{\ell_1, \ell_4, \ell_5, \ell_6\}, 0) \wedge \text{Chk}(\{\ell_2, \ell_3\}, 2) \rightarrow \text{Move}(\ell_4)$
 - Rule16: Buddy = $\ell_0 \wedge \text{Chk}(\{\ell_1, \ell_2, \ell_5, \ell_6\}, 0) \wedge \neg \text{Chk}(\ell_3, 0) \wedge \text{Chk}(\ell_4, 2) \rightarrow \text{Move}(\ell_5)$
 - Rule17: Buddy = $\ell_0 \wedge \text{Chk}(\{\ell_1, \ell_2, \ell_3, \ell_6\}, 0) \wedge \neg \text{Chk}(\ell_4, 0) \wedge \text{Chk}(\ell_5, 2) \rightarrow \text{Move}(\ell_6)$
 - Rule18: Buddy = $\ell_0 \wedge \text{Chk}(\{\ell_1, \ell_2, \ell_3, \ell_4\}, 0) \wedge \text{Chk}(\{\ell_5, \ell_6\}, 2) \rightarrow \text{Move}(\ell_1)$
 - Rule19: Buddy = $\ell_2 \wedge \text{Chk}(\{\ell_3, \ell_4, \ell_5\}, 0) \wedge \text{Chk}(\{\ell_0, \ell_2\}, 1) \wedge \text{Chk}(\{\ell_1, \ell_6\}, 2) \rightarrow \text{Move}(\ell_2)$
 - Rule20: Buddy = $\ell_4 \wedge \text{Chk}(\{\ell_1, \ell_5, \ell_6\}, 0) \wedge \text{Chk}(\ell_4, 1) \wedge \text{Chk}(\{\ell_2, \ell_3\}, 2) \rightarrow \text{Move}(\ell_4)$
 - Rule21: Buddy = $\ell_6 \wedge \text{Chk}(\{\ell_1, \ell_2, \ell_3\}, 0) \wedge \neg \text{Chk}(\ell_4, 0) \wedge \text{Chk}(\ell_5, 2) \wedge \text{Chk}(\ell_6, 1) \rightarrow \text{Move}(\ell_6)$
 - Rule22: Buddy = $\ell_1 \wedge \text{Chk}(\{\ell_3, \ell_4, \ell_5, \ell_6\}, 0) \wedge \text{Chk}(\{\ell_0, \ell_1, \ell_2\}, 1) \rightarrow \text{Move}(\ell_1)$
 - Rule23: Buddy = $\ell_2 \wedge \text{Chk}(\{\ell_1, \ell_4, \ell_5, \ell_6\}, 0) \wedge \text{Chk}(\{\ell_0, \ell_2, \ell_3\}, 1) \rightarrow \text{Move}(\ell_2)$
 - Rule24: Buddy = $\ell_3 \wedge \text{Chk}(\{\ell_1, \ell_2, \ell_5, \ell_6\}, 0) \wedge \text{Chk}(\{\ell_0, \ell_3, \ell_4\}, 1) \rightarrow \text{Move}(\ell_3)$
 - Rule25: Buddy = $\ell_4 \wedge \text{Chk}(\{\ell_1, \ell_2, \ell_3, \ell_6\}, 0) \wedge \text{Chk}(\{\ell_0, \ell_4, \ell_5\}, 1) \rightarrow \text{Move}(\ell_4)$
-

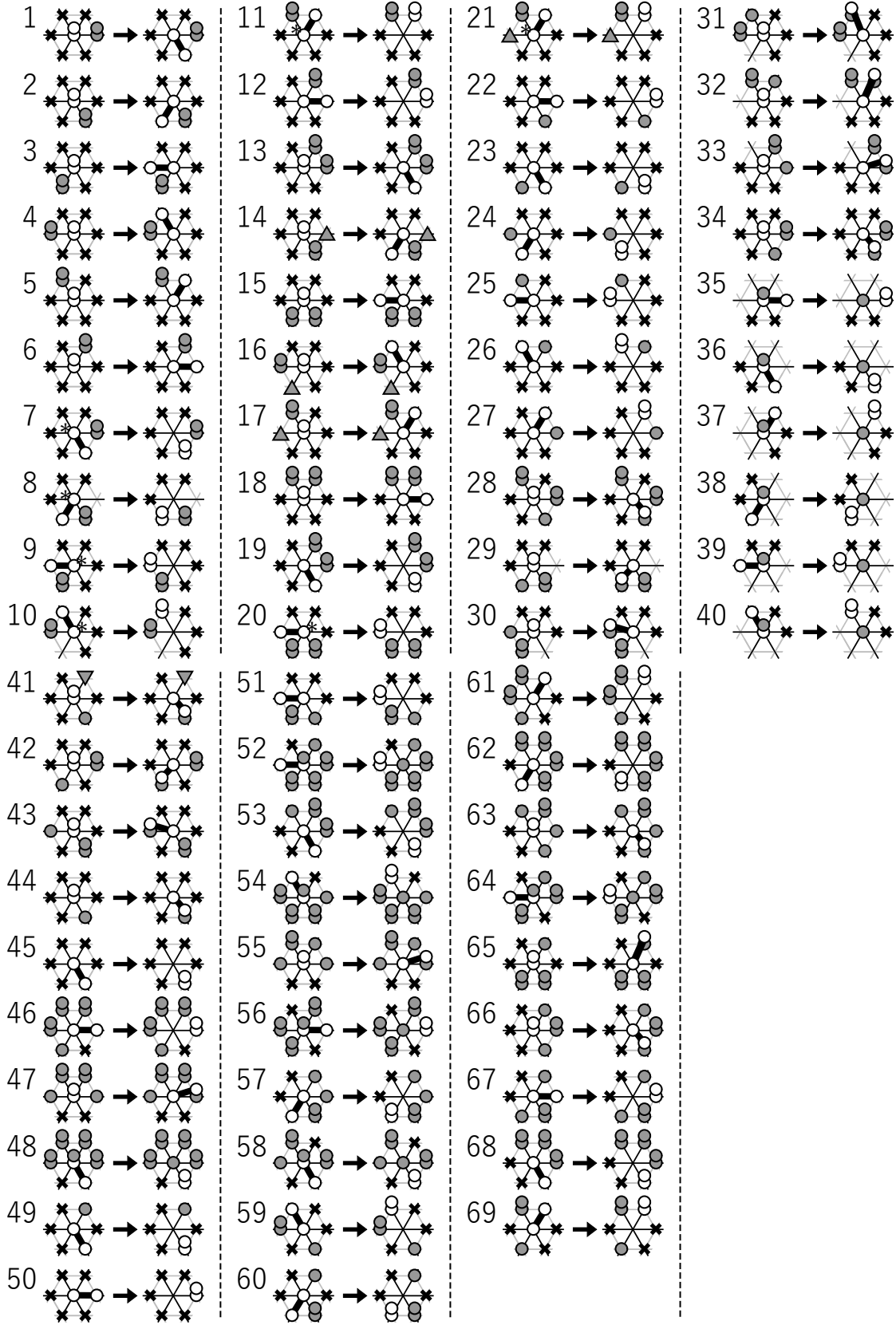


Figure 27: The proposed algorithm for the 7-pairbots-gathering

-
- Rule26: $\text{Buddy} = l_5 \wedge \text{Chk}(\{l_1, l_2, l_3, l_4\}, 0) \wedge \text{Chk}(\{l_0, l_5, l_6\}, 1) \rightarrow \text{Move}(l_5)$
 Rule27: $\text{Buddy} = l_6 \wedge \text{Chk}(\{l_2, l_3, l_4, l_5\}, 0) \wedge \text{Chk}(\{l_0, l_1, l_6\}, 1) \rightarrow \text{Move}(l_6)$
 Rule28: $\text{Buddy} = l_0 \wedge \text{Chk}(\{l_3, l_4, l_6\}, 0) \wedge \text{Chk}(l_2, 1) \wedge \text{Chk}(\{l_1, l_5\}, 2) \rightarrow \text{Move}(l_2)$
 Rule29: $\text{Buddy} = l_0 \wedge \text{Chk}(\{l_4, l_5, l_6\}, 0) \wedge \text{Chk}(l_3, 1) \wedge \text{Chk}(l_2, 2) \rightarrow \text{Move}(l_3)$
 Rule30: $\text{Buddy} = l_0 \wedge \text{Chk}(\{l_1, l_5, l_6\}, 0) \wedge \text{Chk}(l_4, 1) \wedge \text{Chk}(l_3, 2) \rightarrow \text{Move}(l_4)$
 Rule31: $\text{Buddy} = l_0 \wedge \text{Chk}(\{l_1, l_2, l_6\}, 0) \wedge \text{Chk}(l_5, 1) \wedge \text{Chk}(l_4, 2) \rightarrow \text{Move}(l_5)$
 Rule32: $\text{Buddy} = l_0 \wedge \text{Chk}(\{l_1, l_2, l_3\}, 0) \wedge \text{Chk}(l_6, 1) \wedge \text{Chk}(l_5, 2) \rightarrow \text{Move}(l_6)$
 Rule33: $\text{Buddy} = l_0 \wedge \text{Chk}(\{l_2, l_3, l_4\}, 0) \wedge \text{Chk}(l_1, 1) \wedge \text{Chk}(l_6, 2) \rightarrow \text{Move}(l_1)$
 Rule34: $\text{Buddy} = l_0 \wedge \text{Chk}(\{l_3, l_4, l_5, l_6\}, 0) \wedge \text{Chk}(l_2, 1) \wedge \text{Chk}(l_1, 2) \rightarrow \text{Move}(l_2)$
 Rule35: $\text{Buddy} = l_1 \wedge \text{Chk}(\{l_2, l_3\}, 0) \wedge \text{Chk}(l_1, 1) \wedge \text{Chk}(l_0, 2) \rightarrow \text{Move}(l_1)$
 Rule36: $\text{Buddy} = l_2 \wedge \text{Chk}(\{l_3, l_4\}, 0) \wedge \text{Chk}(l_2, 1) \wedge \text{Chk}(l_0, 2) \rightarrow \text{Move}(l_2)$
 Rule37: $\text{Buddy} = l_6 \wedge \text{Chk}(\{l_1, l_2\}, 0) \wedge \text{Chk}(l_6, 1) \wedge \text{Chk}(l_0, 2) \rightarrow \text{Move}(l_6)$
 Rule38: $\text{Buddy} = l_3 \wedge \text{Chk}(\{l_4, l_5\}, 0) \wedge \text{Chk}(l_3, 1) \wedge \text{Chk}(l_0, 2) \rightarrow \text{Move}(l_3)$
 Rule39: $\text{Buddy} = l_4 \wedge \text{Chk}(\{l_5, l_6\}, 0) \wedge \text{Chk}(l_4, 1) \wedge \text{Chk}(l_0, 2) \rightarrow \text{Move}(l_4)$
 Rule40: $\text{Buddy} = l_5 \wedge \text{Chk}(\{l_1, l_6\}, 0) \wedge \text{Chk}(l_5, 1) \wedge \text{Chk}(l_0, 2) \rightarrow \text{Move}(l_5)$
 Rule41: $\text{Buddy} = l_0 \wedge \text{Chk}(\{l_1, l_3, l_4, l_5\}, 0) \wedge \text{Chk}(l_2, 1) \wedge \neg \text{Chk}(l_6, 1) \rightarrow \text{Move}(l_2)$
 Rule42: $\text{Buddy} = l_0 \wedge \text{Chk}(\{l_2, l_4, l_5, l_6\}, 0) \wedge \text{Chk}(l_3, 1) \wedge \text{Chk}(l_1, 2) \rightarrow \text{Move}(l_3)$
 Rule43: $\text{Buddy} = l_0 \wedge \text{Chk}(\{l_1, l_3, l_5, l_6\}, 0) \wedge \text{Chk}(l_4, 1) \wedge \text{Chk}(l_2, 2) \rightarrow \text{Move}(l_4)$
 Rule44: $\text{Buddy} = l_0 \wedge \text{Chk}(\{l_1, l_3, l_4, l_5, l_6\}, 0) \wedge \text{Chk}(l_2, 1) \rightarrow \text{Move}(l_2)$
 Rule45: $\text{Buddy} = l_2 \wedge \text{Chk}(\{l_1, l_3, l_4, l_5, l_6\}, 0) \wedge \text{Chk}(\{l_0, l_2\}, 1) \rightarrow \text{Move}(l_2)$
 Rule46: $\text{Buddy} = l_1 \wedge \text{Chk}(l_2, 0) \wedge \text{Chk}(\{l_0, l_1, l_3\}, 1) \wedge \text{Chk}(\{l_4, l_5, l_6\}, 2) \rightarrow \text{Move}(l_1)$
 Rule47: $\text{Buddy} = l_0 \wedge \text{Chk}(\{l_2, l_3\}, 0) \wedge \text{Chk}(\{l_1, l_4\}, 1) \wedge \text{Chk}(\{l_5, l_6\}, 2) \rightarrow \text{Move}(l_1)$
 Rule48: $\text{Buddy} = l_2 \wedge \text{Chk}(l_3, 0) \wedge \text{Chk}(l_2, 1) \wedge \text{Chk}(\{l_0, l_1, l_4, l_5, l_6\}, 2) \rightarrow \text{Move}(l_2)$
 Rule49: $\text{Buddy} = l_2 \wedge \text{Chk}(\{l_1, l_3, l_4, l_5\}, 0) \wedge \text{Chk}(\{l_0, l_2, l_6\}, 1) \rightarrow \text{Move}(l_2)$
 Rule50: $\text{Buddy} = l_1 \wedge \text{Chk}(\{l_2, l_3, l_4, l_5, l_6\}, 0) \wedge \text{Chk}(\{l_0, l_1\}, 1) \rightarrow \text{Move}(l_1)$
 Rule51: $\text{Buddy} = l_4 \wedge \text{Chk}(\{l_1, l_5, l_6\}, 0) \wedge \text{Chk}(\{l_0, l_2, l_4\}, 1) \wedge \text{Chk}(l_3, 2) \rightarrow \text{Move}(l_4)$
 Rule52: $\text{Buddy} = l_4 \wedge \text{Chk}(l_5, 0) \wedge \text{Chk}(\{l_4, l_6\}, 1) \wedge \text{Chk}(\{l_0, l_1, l_2, l_3\}, 2) \rightarrow \text{Move}(l_4)$
 Rule53: $\text{Buddy} = l_2 \wedge \text{Chk}(\{l_3, l_4\}, 0) \wedge \text{Chk}(\{l_0, l_2, l_5\}, 1) \wedge \text{Chk}(\{l_1, l_6\}, 2) \rightarrow \text{Move}(l_2)$
 Rule54: $\text{Buddy} = l_5 \wedge \text{Chk}(l_6, 0) \wedge \text{Chk}(\{l_1, l_5\}, 1) \wedge \text{Chk}(\{l_0, l_2, l_3, l_4\}, 2) \rightarrow \text{Move}(l_5)$
 Rule55: $\text{Buddy} = l_0 \wedge \text{Chk}(\{l_2, l_3\}, 0) \wedge \text{Chk}(\{l_1, l_4, l_6\}, 1) \wedge \text{Chk}(l_5, 2) \rightarrow \text{Move}(l_1)$
 Rule56: $\text{Buddy} = l_1 \wedge \text{Chk}(\{l_2, l_5\}, 0) \wedge \text{Chk}(l_1, 1) \wedge \text{Chk}(\{l_0, l_3, l_4, l_6\}, 2) \rightarrow \text{Move}(l_1)$
 Rule57: $\text{Buddy} = l_3 \wedge \text{Chk}(\{l_4, l_5\}, 0) \wedge \text{Chk}(\{l_0, l_1, l_3, l_6\}, 1) \wedge \text{Chk}(l_2, 2) \rightarrow \text{Move}(l_3)$
 Rule58: $\text{Buddy} = l_2 \wedge \text{Chk}(\{l_3, l_6\}, 0) \wedge \text{Chk}(\{l_2, l_4\}, 1) \wedge \text{Chk}(\{l_0, l_1, l_5\}, 2) \rightarrow \text{Move}(l_2)$
 Rule59: $\text{Buddy} = l_5 \wedge \text{Chk}(\{l_1, l_3, l_6\}, 0) \wedge \text{Chk}(\{l_0, l_2, l_5\}, 1) \wedge \text{Chk}(l_4, 2) \rightarrow \text{Move}(l_5)$
 Rule60: $\text{Buddy} = l_3 \wedge \text{Chk}(\{l_1, l_4, l_5\}, 0) \wedge \text{Chk}(\{l_0, l_3, l_6\}, 1) \wedge \text{Chk}(l_2, 2) \rightarrow \text{Move}(l_3)$
 Rule61: $\text{Buddy} = l_6 \wedge \text{Chk}(\{l_1, l_2\}, 0) \wedge \text{Chk}(\{l_0, l_3, l_6\}, 1) \wedge \text{Chk}(\{l_4, l_5\}, 2) \rightarrow \text{Move}(l_6)$
 Rule62: $\text{Buddy} = l_3 \wedge \text{Chk}(l_4, 0) \wedge \text{Chk}(\{l_0, l_3\}, 1) \wedge \text{Chk}(\{l_1, l_2, l_5, l_6\}, 2) \rightarrow \text{Move}(l_3)$
 Rule63: $\text{Buddy} = l_0 \wedge \text{Chk}(\{l_3, l_4\}, 0) \wedge \text{Chk}(\{l_1, l_2, l_5\}, 1) \wedge \text{Chk}(l_6, 2) \rightarrow \text{Move}(l_2)$
 Rule64: $\text{Buddy} = l_4 \wedge \text{Chk}(\{l_2, l_5\}, 0) \wedge \text{Chk}(\{l_4, l_6\}, 1) \wedge \text{Chk}(\{l_0, l_1, l_3\}, 2) \rightarrow \text{Move}(l_4)$
 Rule65: $\text{Buddy} = l_0 \wedge \text{Chk}(\{l_1, l_4, l_5\}, 0) \wedge \text{Chk}(l_6, 1) \wedge \text{Chk}(\{l_2, l_3\}, 2) \rightarrow \text{Move}(l_1)$
 Rule66: $\text{Buddy} = l_0 \wedge \text{Chk}(\{l_3, l_4, l_5\}, 0) \wedge \text{Chk}(\{l_2, l_6\}, 1) \wedge \text{Chk}(l_1, 2) \rightarrow \text{Move}(l_2)$
 Rule67: $\text{Buddy} = l_1 \wedge \text{Chk}(\{l_4, l_5\}, 0) \wedge \text{Chk}(\{l_0, l_1, l_3, l_6\}, 1) \wedge \text{Chk}(l_2, 2) \rightarrow \text{Move}(l_1)$
 Rule68: $\text{Buddy} = l_2 \wedge \text{Chk}(\{l_3, l_4\}, 0) \wedge \text{Chk}(\{l_0, l_2\}, 1) \wedge \text{Chk}(\{l_1, l_5, l_6\}, 2) \rightarrow \text{Move}(l_2)$
 Rule69: $\text{Buddy} = l_6 \wedge \text{Chk}(\{l_1, l_2, l_4\}, 0) \wedge \text{Chk}(\{l_0, l_3, l_6\}, 1) \wedge \text{Chk}(l_5, 2) \rightarrow \text{Move}(l_6)$
-

4.4 Correctness of the Proposed Algorithm

The proof of the correctness of the proposed algorithm is very challenging because it includes many rules. However, in this problem, the number of *pairbot* is fixed to 7, all *pairbots* are initially in *short* state, and only *connected* initial configurations are allowed; this implies that there exist only the constant number of initial configurations. Therefore, we implement a simulator (provided at Kim and Taguchi [2023]) for the proposed algorithm which can generate all possible initial configurations; there exist 3,652 initial configurations (as a result from the simulator). Note that the proposed algorithm is deterministic and we assume an FSYNC scheduler, thus there can be only one execution appears when an initial configuration is given. We had checked the proposed algorithm in every initial configuration using the simulation, and the proposed algorithm solves the 7-pairbots-gathering problem from all possible initial configurations. Therefore, the following theorem holds.

Theorem 6 *The proposed algorithm solves the 7-pairbots-gathering problem from any arbitrary connected configuration under an FSYNC scheduler.*

5 Conclusion

In this study, we have introduced a new computational model, the *Pairbot model*, consisting of paired robots that are called *pairbots*, which is based on the *LCM* model Suzuki and Yamashita [1999]. In the proposed model, each *pairbot* repeatedly changes the positional relation of the two robots (i.e., *long* and *short*) to achieve the goal. We presented the *perpetual marching* and the *7-pairbots-gathering* problems to help to understand the computational power of the *Pairbot model*. In particular, from the *perpetual marching* problem, we can clarify the difference of the computational power in terms of a *scheduler*; the problem is solvable by 3 *pairbots* under an ASYNC scheduler, but unsolvable by 6 or less LCM-robots even under an SSYNC scheduler. Moreover, in the *7-pairbots-gathering* problem, we showed the difference of the computational power in terms of a *visibility range*; the problem is solvable by *pairbots* with visibility range 1, but unsolvable by LCM-robots with the same visibility range (visibility range 2 is necessary to solve).

The *Pairbot model* basically has similar variations of assumptions (e.g., scheduler, geometric agreement, visibility, etc.), but it has one big different feature: every robot has one *implicitly distinguishable* robot as its *buddy*. We introduced only two problems here, but we are considering various problems in the *Pairbot model* such as pattern formation (a line, a triangle, or a hexagon), filling problem, and uniform deployment, as the future work. Especially, we are interested in the problems which have been solved in other computational models such as *Amoebot*, *SILBOT*, and *MOBLOT* to clarify the difference between *Pairbot model* and these computational models for PM.

The *pairbot* and the conventional *LCM*-models have many common features, thus, we can consider the simulation of the *Pairbot model* using the *LCM* model with some additional capabilities (e.g., light Das et al. [2015]). Clarifying the minimum required capabilities for the *LCM* model to simulate the *Pairbot model* is another future work.

References

- Ichiro Suzuki and Masafumi Yamashita. Distributed anonymous mobile robots: Formation of geometric patterns. *SIAM Journal on Computing*, 28(4):1347–1363, 1999.
- Shantanu Das, Paola Flocchini, Giuseppe Prencipe, and Masafumi Yamashita. Autonomous mobile robots with lights. *Theoretical Computer Science*, 609, 09 2015.
- Paola Flocchini, Giuseppe Prencipe, and Nicola Santoro, editors. *Distributed Computing by Mobile Entities, Current Research in Moving and Computing*, volume 11340 of *Lecture Notes in Computer Science*. Springer, 2019. ISBN 978-3-030-11071-0.
- Giuseppe Prencipe. Autonomous mobile robots: A distributed computing perspective. volume 8243, pages 6–21, 12 2014.
- S. Cicerone, Di Stefano, and A. Navarra. Gathering of robots on meeting-points. *Distributed Computing*, 31(1):1–50, 2018.
- M. Cieliebak, P. Flocchini, G. Prencipe, and N. Santoro. Distributed computing by mobile robots: Gathering. *SIAM Journal on Computing*, 41(4):829–879, 2012.
- Paola Flocchini, Giuseppe Prencipe, Nicola Santoro, and Peter Widmayer. Arbitrary pattern formation by asynchronous, anonymous, oblivious robots. *Theoretical Computer Science*, 407:412–447, 11 2008.
- Paola Flocchini, Giuseppe Prencipe, Nicola Santoro, Peter Widmayer, Alok Aggarwal, and C. Rangan. Hard tasks for weak robots: The role of common knowledge in pattern formation by autonomous mobile robots. volume 1741, pages 93–102, 01 1999.

- N. Fujinaga, Y. Yamauchi, H. Ono, S. Kijima, and M. Yamashita. Pattern formation by oblivious asynchronous mobile robots. *SIAM Journal on Computing*, 44(3):740–785, 2015.
- Y. Yamauchi, T. Uehara, S. Kijima, and M. Yamashita. Plane formation by synchronous mobile robots in the three-dimensional euclidean space. *Journal of the ACM*, 64:3(16):16:1–16:43, 2017.
- V. Gervasi and G. Prencipe. Coordination without communication: The case of the flocking problem. *Discrete Applied Mathematics*, 144(3):324–344, 2004.
- S. Souissi, T. Izumi, and K. Wada. Oracle-based flocking of mobile robots in crash-recovery model. In *Proceedings of the 11th International Symposium on Stabilization, Safety, and Security of Distributed Systems (SSS)*, pages 683–697, 2009.
- Taisuke Izumi, Samia Souissi, Yoshiaki Katayama, Nobuhiro Inuzuka, Xavier Défago, Koichi Wada, and Masafumi Yamashita. The gathering problem for two oblivious robots with unreliable compasses. *SIAM Journal on Computing*, 41, 11 2011.
- Ajay D. Kshemkalyani, Anisur Rahaman Molla, and Gokarna Sharma. Efficient dispersion of mobile robots on dynamic graphs. In *2020 IEEE 40th International Conference on Distributed Computing Systems (ICDCS)*, pages 732–742, 2020. doi:10.1109/ICDCS47774.2020.00100.
- Anisur Rahaman Molla, Kaushik Mondal, and William K. Moses. Byzantine dispersion on graphs. In *2021 IEEE International Parallel and Distributed Processing Symposium (IPDPS)*, pages 942–951, 2021. doi:10.1109/IPDPS49936.2021.00103.
- John Augustine and William K. Moses. Dispersion of mobile robots: A study of memory-time trade-offs. In *Proceedings of the 19th International Conference on Distributed Computing and Networking, ICDCN '18*, New York, NY, USA, 2018. Association for Computing Machinery. ISBN 9781450363723. doi:10.1145/3154273.3154293. URL <https://doi.org/10.1145/3154273.3154293>.
- Lali Barriere, Paola Flocchini, Eduardo Mesa-Barrameda, and Nicola Santoro. Uniform scattering of autonomous mobile robots in a grid. In *2009 IEEE International Symposium on Parallel and Distributed Processing*, pages 1–8, 2009. doi:10.1109/IPDPS.2009.5160871.
- Jurek Czyzowicz, Leszek Gasieniec, and Andrzej Pelc. Gathering few fat mobile robots in the plane. *Theor. Comput. Sci.*, 410(6-7):481–499, 2009. doi:10.1016/j.tcs.2008.10.005. URL <https://doi.org/10.1016/j.tcs.2008.10.005>.
- Aisha Aljohani, Pavan Poudel, and Gokarna Sharma. Complete visitability for autonomous robots on graphs. In *2018 IEEE International Parallel and Distributed Processing Symposium (IPDPS)*, pages 733–742, 2018. doi:10.1109/IPDPS.2018.00083.
- Yonghwan Kim, Yoshiaki Katayama, and Koichi Wada. Asynchronous complete visibility algorithm for luminous robots on grid. In *Eleventh International Symposium on Computing and Networking, CANDAR 2023 - Workshops, Matsue, Japan, November 27-30, 2023*, pages 107–113. IEEE, 2023. doi:10.1109/CANDARW60564.2023.00026. URL <https://doi.org/10.1109/CANDARW60564.2023.00026>.
- Kevin Buchin, Paola Flocchini, Irina Kostitsyna, Tom Peters, Nicola Santoro, and Koichi Wada. Autonomous mobile robots: Refining the computational landscape. In *2021 IEEE International Parallel and Distributed Processing Symposium Workshops (IPDPSW)*, pages 576–585, 2021. doi:10.1109/IPDPSW52791.2021.00091.
- Tommaso Toffoli and Norman Margolus. Programmable matter: Concepts and realization. *Int. J. High Speed Comput.*, 5(2):155–170, 1993.
- Seth Copen Goldstein, Jason D. Campbell, and Todd C. Mowry. Programmable matter. *IEEE Computer*, 38(6):99–101, Jun 2005.
- Josh C. Bongard. Evolutionary robotics. *Communications of ACM*, 56(8):74–83, 2013. ISSN 0001-0782.
- Sangbae Kim, Cecilia Laschi, and Barry Trimmer. Soft robotics: a bioinspired evolution in robotics. *Trends in Biotechnology*, 31(5):287–294, 2013. ISSN 0167-7799.
- Gianfranco Cerofolini, Paolo Amato, Massimo Masserini, and Giancarlo Mauri. A surveillance system for early-stage diagnosis of endogenous diseases by swarms of nanobots. *Advanced Science Letters*, 3:345–352, 12 2010. doi:10.1166/asl.2010.1138.
- A. L. Yarin. Nanofibers, nanofluidics, nanoparticles and nanobots for drug and protein delivery systems. *Scientia Pharmaceutica*, 78(3):542–542, 2010. ISSN 2218-0532.
- Zahra Derakhshandeh, Shlomi Dolev, Robert Gmyr, Andréa Richa, Christian Scheideler, and Thim Strothmann. Brief announcement: Amoebot-a new model for programmable matter. *Annual ACM Symposium on Parallelism in Algorithms and Architectures*, 06 2014.

- Joshua Daymude, Zahra Derakhshandeh, Robert Gmyr, Alexandra Porter, Andréa Richa, Christian Scheideler, and Thim Strothmann. On the runtime of universal coating for programmable matter. *Natural Computing*, 17, 11 2017a.
- Rida A. Bazzi and Joseph L. Briones. Stationary and deterministic leader election in self-organizing particle systems. In Mohsen Ghaffari, Mikhail Nesterenko, Sébastien Tixeuil, Sara Tucci, and Yukiko Yamauchi, editors, *Stabilization, Safety, and Security of Distributed Systems - 21st International Symposium, SSS 2019, Pisa, Italy, October 22-25, 2019, Proceedings*, volume 11914 of *Lecture Notes in Computer Science*, pages 22–37. Springer, 2019.
- Joshua J. Daymude, Robert Gmyr, Andréa W. Richa, Christian Scheideler, and Thim Strothmann. Improved leader election for self-organizing programmable matter. In Antonio Fernández Anta, Tomasz Jurdzinski, Miguel A. Mosteiro, and Yanyong Zhang, editors, *Algorithms for Sensor Systems - 13th International Symposium on Algorithms and Experiments for Wireless Sensor Networks, ALGOSENSORS 2017, Vienna, Austria, September 7-8, 2017, Revised Selected Papers*, volume 10718 of *Lecture Notes in Computer Science*, pages 127–140. Springer, 2017b.
- Joshua Daymude, Robert Gmyr, Kristian Hinnenthal, Irina Kostitsyna, Christian Scheideler, and Andréa Richa. Convex hull formation for programmable matter. pages 1–10, 01 2020.
- Joshua J. Daymude, Andréa W. Richa, and Christian Scheideler. The canonical amoebot model: Algorithms and concurrency control. In Seth Gilbert, editor, *35th International Symposium on Distributed Computing, DISC 2021, October 4-8, 2021, Freiburg, Germany (Virtual Conference)*, volume 209 of *LIPIcs*, pages 20:1–20:19. Schloss Dagstuhl - Leibniz-Zentrum für Informatik, 2021.
- Gianlorenzo D’Angelo, Mattia D’Emidio, Shantanu Das, Alfredo Navarra, and Giuseppe Prencipe. Asynchronous silent programmable matter achieves leader election and compaction. *IEEE Access*, 8:207619–207634, 2020.
- Serafino Cicerone, Alessia Di Fonso, Gabriele Di Stefano, and Alfredo Navarra. MOBLot: molecular oblivious robots. In Frank Dignum, Alessio Lomuscio, Ulle Endriss, and Ann Nowé, editors, *AAMAS ’21: 20th International Conference on Autonomous Agents and Multiagent Systems, Virtual Event, United Kingdom, May 3-7, 2021*, pages 350–358. ACM, 2021.
- Giuseppe Antonio Di Luna, Paola Flocchini, Nicola Santoro, Giovanni Viglietta, and Yukiko Yamauchi. Shape formation by programmable particles. *Distributed Comput.*, 33(1):69–101, 2020.
- Zahra Derakhshandeh, Robert Gmyr, Andréa W. Richa, Christian Scheideler, and Thim Strothmann. An algorithmic framework for shape formation problems in self-organizing particle systems. In Faramarz Fekri, Sasitharan Balasubramaniam, Tommaso Melodia, Ahmad Beirami, and Albert Cabellos, editors, *Proceedings of the Second Annual International Conference on Nanoscale Computing and Communication, NANOCOM’ 15, Boston, MA, USA, September 21-22, 2015*, pages 21:1–21:2. ACM, 2015.
- Masahiro Shibata, Masaki Ohyabu, Yuichi Sudo, Junya Nakamura, Yonghwan Kim, and Yoshiaki Katayama. Visibility-optimal gathering of seven autonomous mobile robots on triangular grids. *International Journal of Networking and Computing*, 12(1):2–25, 2022.
- Yonghwan Kim and Yuya Taguchi. 7-pairbots-gathering algorithm simulator and verifier, 2023. URL <https://github.com/chaika1015/7pairbot-gathering>.